Design and analysis of UFLS scheme for a low-inertia based power grid

A thesis submitted to Macquarie University
for the degree of Master of Research
Department of Engineering

By

S K Sazzad Hossain

Macquarie ID: 45033137

MRes Student, School of Engineering

The work presented in this thesis was carried out at the School of Engineering, Macquarie University, Sydney, Australia, between January 2018 and October 2018. This work was principally supervised by Associate Professor Jahangir Hossain. Except where acknowledged in the customary manner, the material presented in this thesis is, to the best of my knowledge, original and has not been submitted in whole or part for a degree in any other university or institution other than Macquarie University.

_____

S K Sazzad Hossain

List of Acronym

AUFLS	Adaptive Under Frequency Load Shedding
ANN	Artificial Neural Network
BESS	Battery Energy Storage System
DER	Distributed energy resource
DFIG	Double-fed induction generator
EPS	Energy Power System
ESS	Energy Storage System
FFTD	Frequency first time Derivative
FSTD	Frequency second time Derivative
FLLSC	Fuzzy Logic Load Shed Controller
GSF	Generation Shift Factor
GTBKTT	Gradient Technique Based on Kuhn-Tucker Theorem
ILS	Intelligent Load Shedding Scheme
IHSA	Improved Harmony Search Algorithm
LSCM	Load Shedding Controller Module
LSA	Load Shedding Amount
LSA	Load Shedding Amount
LODF	Line Outage Distribution Factor
NNCA	Nearest neighbour consensus
OFI	Over-frequency index
PSO	Particle Swarm Optimiser
PMU	Phasor Measurement Unit
PLC	Power-Line Communication
PLN	Piecewise-linear nose curve
PSO	Particle-Swarm Optimiser
ROCOF	Rate of Change of Frequency

SFR	System Frequency Response
SFR	System Frequency Response
SMIB	Single Machine Infinite Bus
SI	Synthetic Inertia
TLBO	Teaching-learning based optimisation
UVI	Under-voltage index
UFI	Under-frequency index
UFLS	Under-frequency Load Shedding
WPP	Wind Power Plant
WAMS	Wide-Area Monitoring System

ABSTRACT

Due to the high penetrations of renewable energy sources, a significant change to power systems' dynamic behavior following a contingency event has become a major concern in modern days. A Power system's inertia is getting weaker with the integrations of renewable generators. As a result, UFLS schemes may fail to protect the frequency decline below the threshold limits with conventional settings. Inadequate load shedding during frequency excursion process may lead a cascade tripping of remaining generators, leading to a possible blackout.

This thesis addresses this problem and analyses the impacts of penetration of renewable energies into grid. Here, a modified load-shedding method is proposed by considering ROCOF and the total system's damping factor. Then, it models the under-frequency relay by using MILP techniques to provide complete freedom of relays while dealing with the same problem. Furthermore, this thesis also shows a comparison of performances of these three techniques (conventional, proposed and MILP). Here, a 13-bus network from real power system is considered as a test system and several case studies are conducted using the PSS/E. From simulations it is found that the proposed on-line based UFLS scheme is more efficient and one of the promising solutions to avoid blackouts

Acknowledgments

First and foremost, I thank the almighty Allah for showing me the paths and giving me the opportunity to successfully complete this degree. I am highly grateful to several individuals for their guidance and assistance to make this thesis possible. I would like to express my sincere gratitude and appreciation to my principal supervisor, A/Professor Jahangir Hossain, for selecting me to work under his supervision. His excellent guidance, patience, and valuable advice helped me to learn a lot. I would also like to express my sincere thanks and admiration to my group mates, for their helpful instructions, support, and frequent meetings to solve the technical problems.

I would also like to thank Dr Keith Imrie for his proofreading and valuable feedback in improving the quality of this thesis. I wish to acknowledge Macquarie University for awarding me the international Research Training Pathway (iRTP) scholarship and providing me with financial supports.

Finally, special thanks and cordial love to my family. I must dedicate this work to my parents, whose constant support, prayers and encouragement allowed me to start and complete this academic goal.

List of Publications

S. S. Hossain, M.J Hossain, Edstan Fernandez and Md Shihanur Rahman "Design and analysis of an UFLS scheme for low-inertia based power grid" in proc. of the Australasian Universities Power Engineering Conference 2018 (AUPEC 2018), November 27 ~ 30, 2018, The University of Auckland, New Zealand.

Table of Contents

List of Figures

List of Tables

Chapter 1

Introduction

1.1 Background

In recent years, to ensure energy sustainability as well as to reduce carbon emission, the integration of large-scale intermittent converter-connected renewable energy sources (e.g. photovoltaic (PV), double-fed induction generator (DFIG), wind turbine etc.) have become an essential part in the electric power system. However, the inclusion of renewable energy sources is causing a reduction in system inertia, making the power system more vulnerable to power outages. As a result, the necessity of reliable protection systems has become essential for the power industry more than ever.

Generators in a power system are very sensitive to frequency response and any sudden drop of frequency beyond the threshold limit can cause an instantaneous trip. Trip of any generator in a certain power system may lead to a cascade tripping due to its frequency declination, resulting in a blackout. To avoid this kind of unintentional tripping due to frequency declination, the system's frequency must be maintained within a safe limit.

Frequency stability can be defined by the ability of a power system to maintain a stable frequency response following several contingencies [3]. Power mismatch between the generation and consumption is the main reason that causes the system's frequency to decline. In case of a weak inertia-based system, frequency declination is much more significant than that of a strong inertia-based system. As the system's strength becomes weaker with the penetrations of renewable energy sources, maintaining frequency stability becomes one of the major challenges in the modern power system. The most used technology for maintaining frequency stability is under frequency load shedding (UFLS). Insufficient UFLS can cause the frequency to decline rapidly, leading to a cascade tripping of generators in a system leading to a blackout.

Load shedding and blackout frequently occur in developing countries. For example, the blackout on 1st Nov 2014 in Bangladesh happened due to a sudden generators' outage and insufficient spinning reserves. As a result, the frequency dropped down to 48.9 Hz within 6.86 sec after 444 MW tripping of imported power at (High Voltage Direct Current) HVDC system [4]. As this event took place in peak time, the existing settings of five stages of UFLS were insufficient to arrest the frequency decline within the safe time limit of the generators protection limit, resulting in a system blackout. Another blackout due to insufficient load shedding took place in San Diego region in 2011. This blackout was the consequence of power outage in the Pacific Southwest. In

September 2016 South Australia faced a major power outage (except the Kangaroo Island) due to a damage in transmission networks caused by a natural calamity.

The above-mentioned historical events depict the importances of designing an appropriate UFLS scheme to ensure a reliable and stable power system. But the design of a UFLS scheme has become more complex and challenging due to the integration of renewable energy sources. As the conventional UFLS schemes have proved to be less effective, so it is significantly importan to design new under frequency protection schemes which can overcome the deficiencies of the existing models and thereby increase the system's reliability to a great extent.

This thesis discusses the existing methods of under-frequency load shedding and analyses the importance of including a system's inertia on the designing of UFLS scheme. To do that, a conventional UFLS scheme is developed, and its performance with the penetration of renewable energy is thoroughly investigated. Then, an online based under frequency load shedding scheme is designed and implemented to overcome the deficiencies of conventional load shedding schemes in the presence of renewable sources. The proposed load-shedding scheme is tested on a 13-bus real power network, which is a portion of the Bangladesh power grid. To show the comparison of the proposed on-line base UFLS scheme besides the conventional scheme, another off-line based method which includes mixed-integer linear programming (MILP)[6] is designed and implemented in this research.

1.2 Recent Advances in the Design of UFLS Programs

Problems regarding UFLS was first studied by the Operating Committee of the North West Power Pool in 1950. Since then a lot of work has been done to optimise the UFLS to avoid power outages and thus improve the system's reliability. But impact of renewable energy penetrations on UFLS are discussed in only a few research projects.

In the last decades, several researches on optimisation of UFLS scheme have been carried out. An un-optimised UFLS scheme can lead a system into many undesirable conditions like frequency overshoot, over-voltage, or under-voltage which can cause a system blackout. A model was proposed following the optimisation of the System frequency response (SFR) for a large power system in [4]. To optimise the SFR model, the response of governors-prime movers and the dynamic characteristics of the load were considered. Then by using the Particle swarm optimisation (PSO) algorithm, a UFLS scheme was designed. This inertia-based research may face difficulties in optimising load shedding amount with the injections of renewable energy sources.

Load-shedding has an impact on a system's reliability, so to minimise the Load-Shedding Amount (LSA), another method is proposed in[15] based on online and real-time study. In this research, an online study was performed to determine the piecewise-

linear nose curve (PLN) to see the load-voltage characteristic, and the droop method was employed to calculate the frequency deviation due to active power changes. During a contingency load voltage and bus frequency were monitored in the real-time study. Then by using the PLN and a frequency droop characteristic curve, under-voltage index (UVI), under-frequency index (UFI), and over-frequency index (OFI) were determined. LSA is finally estimated using those indices. In this research, instead of using conventional linear sensitivity for the load-voltage and load-power characteristics, online and real-time study were used to define the load-voltage load-power relations, which helps to optimise LSA in real scenarios. Probably inclusion of integrated renewable energy sources into their test network could make a difference in the frequency droop characteristics which may have an impact in determining the actual LSA.

In [16] another technique of load-shedding optimisation was proposed based on a teaching-learning procedure called TLBO. Later this optimisation technique was compared with the IHSA and GTBKTT optimisation algorithms. In the proposed algorithm the load-shedding amount (total), voltage stability maximisation and load ability enhancement were set as objective functions and, by meeting these objectives, partial and total blackout was avoided. Though this research describes a new method of avoiding blackout, the impacts of renewable energy penetration on the proposed scheme were absent.

In [17] a smart integrated adaptive centralised control method was proposed by controlling renewable energy sources to minimise the UFLS. Here, the rate of change of frequency (ROCOF) was measured from the Phasor Measurement Unit (PMU). Due to a sudden interruption in the power system the ROCOF drops down significantly. The proposed controller captured the minimum value of the ROCOF and it was used to calculate the amount of power imbalance. When the frequency falls below a pre-set value the imbalanced amount of power was fed from the renewable energy sources. Then after starting the standby diesel generator, the breaker of renewable energy sources went off and the diesel generator started to supply the network.

Designing a proper UFLS scheme depends on proper load-shedding modelling which is related to a system's dynamic characteristics. By adopting an appropriate UFLS model, cascade tripping of generators can be avoided. In 2016, dynamic multi-stage under-frequency load shedding was proposed by considering the uncertainty of generation loss[18]. Here the authors claimed that by counting the uncertainty of generation loss the system frequency can have a better response than the deterministic UFLS scheme. The deterministic UFLS scheme may fail to arrest a frequency decline

due to the uncertainty of generation loss during the UFLS. By adopting the point-estimated method in the design of the UFLS scheme it can be minimized, but even by using the probabilistic method an oscillation in frequency response is noticeable after frequency arresting, which is undesirable. These oscillations last for 15-20 seconds. However, this problem can be solved by replacing the load-shedding scheme with a new scheme using external energy sources (e.g. PV, Wind Power, BESS etc.).

Due to the complex nature of the modern power structure, the existing network protection schemes should be upgraded. To upgrade the Electric Power System (EPS) protection system and to avoid unwanted load-shedding, a Wide-Area Monitoring System (WAMS) based UFLS was proposed in[19].

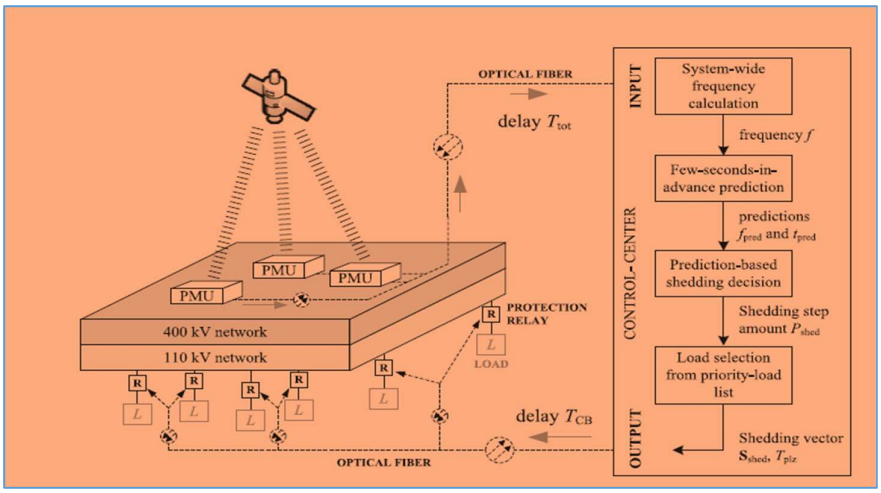

Figure 1 Wide-Area monitoring system WAMS- based UFLS used by [19].

To minimise the errors in the traditional predefined UFLS scheme WAMS gets real-time frequency data from the Phasor Measurement Unit (PMU) and predicts the frequency decline rate through a rough estimation. Predictive load-shedding settings were designed based on two scenarios: one was for the convex frequency period (where the predicted frequency can't be found), load shedding for this instance was carried out only when the system frequency was expected to drop below the violation level very soon otherwise load shedding was delayed. Another scenario was a concave frequency trajectory, where the frequency variation is possible to estimate. Here, loads are shed if the predicted frequency drops down to the violation level. Moreover, lower frequency (predicted) and less time to reach the violation point means more load is ordered to disconnect in the upcoming steps. This method is solely dependent on getting real information from the network, which removes the problems associated with the over-shedding but poses a problem with the execution time delay of the load-shedding process, as additional time delay is added by the relay pickup and the breaker

operation time. Nowadays, the system inertia is reduced significantly, which may not allow us much time to predict and for the designed load-shedding to execute. Therefore, an alternative solution is necessary to improve the design of an Energy Protection System (EPS).

Researchers are trying to develop new control schemes for utilising renewable energy sources to avoid the dependency on a system's inertia in UFLS modeling. A power system's inertia-independent based new method was proposed in [20] by considering power generation variations during the load-shedding process. For the implementation of the proposed scheme, a hybrid distribution system including Fuel Cell (FC), Distributed energy resources (DER), Photovoltaic cell (PV) and Battery energy-storage system (BESS) was chosen and the power deficit was estimated by using the first derivative of the frequency. In this method, the system's initial load shedding was calculated by using the primary estimated system inertia but for distributed power generating units and by considering the possibility of changing the distributed generations' composition the following load-shedding amount was evaluated using the instant frequency gradient before and after load shedding by-

$$P_{d-new} = P_{d-old} + \frac{2H_{eq}}{f_N} .\triangle f'_{Hz} \qquad | t = t_{ch} \tag{1.1}$$

$$H_{eqi} = \frac{f_N \times P_{sh_{i-1}}}{2(f'_{a_{i-1}} - f'_{b_{i-1}})} \tag{1.2}$$

where

$$f'_{a_{i-1}} = frequency\ derivative\ immediately\ after\ the\ i^{th}\ load\ shedding$$

$$f'_{b_{i-1}} = frequency\ derivative\ immediately\ before\ the\ i^{th}\ load\ shedding$$

The proposed UFLS scheme was successfully arrested frequency decline due to the additional power deficit during the frequency-excursion process. The load bus for the first-stage load shedding was determined by measuring the local and neighboring DER units' ability to feed power for local demand. Then, after selection of the buses (to be shed), the load-shedding amount was determined as:

$$\triangle P^{stage1}{}_{shed,j} = (\triangle f_{D,j}.P^{net}_{D,J} / \sum_{j=1}^{ns} \triangle f_{D,j}.P^{net}_{D,J}).\triangle P^{stage1}_{shed} \tag{1.3}$$

$$\triangle P^{stage1}{}_{shed,jd-new} = \text{Curtailment of load at bus} - j \text{ in 1st stage}$$

$$P^{net}_{D,J} = \text{net power injectionat bus} - j$$

$$\triangle f_{D,j} = \text{frequency deviation at bus} - j$$

Then, the second stage of load shedding was determined by the steady-state frequency deviation of the first stage and by the recovery characteristic embedded in the islanded

microgrid. The second-stage load shedding considered the load priorities. Though this research proposed a two-stage load-shedding scheme to arrest frequency decline in the islanded condition, it didn't provide the impact of the voltage fluctuation at the load buses during the UFLS process. Two types of frequency-control strategy were discussed in [21]. One is by estimating the amount of required power from the network frequency and ROCOF data and removing the same amount of load by the 1-stage and 2-stage UFLS scheme, another one is by using droop control for the energy-storage system.

Apart from minimising and rescheduling a load-shedding model, for large power systems an intelligent controlled islanding scheme based on three conditions, i.e., offline, online and real-time monitoring was proposed [22]. The determining factor of islanding was a minimum power flow. In [23] by considering the stability margin of subsystems after islanding a controlled islanding scheme was proposed. By conducting momentary study of the post-fault power system and following the estimation of the constancy limitations of the post-islanding electrical island, an islanding operation was performed. An algorithm was used to separate the healthy zone from the faulty ones to avoid cascade tripping of further generator in [24]. By studying DC load flow and different sensitivity factors like Line Outage Distribution Factors (LODF) and Generation Shift Factors (GSF), the overloads due to an outage was calculated. Thus, the determination of the islanded zone was made based on overload factors. Then for the islanded network a stability analysis was performed, and during any instability conditions an under-voltage load-shedding was performed to bring back to the stability. In [25] a case study was reported on the Pilsen city power distribution system during an islanded operation. It also depicted the impact of frequency and voltage changes during islanding. A comparison between the UFLS and the use of ROCOF on the frequency-excursion process was shown in this research. The integration of the use of ROCOF with the strict second level UFLS scheme can be a more sophisticated approach than using the strict UFLS scheme. But still a sharp fall in frequency may not be recognised by a pre-set ROCOF value, which could lead a blackout.

Transient frequency stability can be achieved by using a Battery Energy Source System (BESS). A new approach to ensure transient stability was proposed in [26] by using a battery as an external energy source. In this paper battery charging-discharging was controlled by measuring the frequency deviations. In addition to that, DC-side faults were studied to find the impact of BESSs in achieving an AC system's stability. This research work can be utilised in minimising the UFLS scheme. The frequency excursion was limited by using the synthetic inertia of Wind Power Plants (WPPs) [27]. In this research the imbalanced active power was supplied by controlling the WPPs inertial response. Two types of control strategies were used here; one is based

on ROCOF and the other is based on the frequency deviation. The limitation of using the doubly-fed induction generator (DFIG) is overcome by using the Synthetic Inertia (SI) controller, which gives a quick response to the frequency-excursion process.

Features of smart appliances can be used to maintain the balance between generator and consumption. To do that a wide-area measurement system is needed. With the progress of demand-response technologies and the application of smart appliances, a novel direction to load-shedding methods emerges under the background of the smart grid [28]. This research used the concept of controlling the operating mechanism of refrigerators and water heaters. This method was tested on an IEEE-39 bus system. This user-dependent model needs the actual participation of user loads, which is often unpredictable. A new approach to an emergency load-shedding scheme was proposed in [29] considering the importance of loads. The priorities of loads to be shed was planned on a feeder basis by the distribution authorities. The proposed scheme was verified on an improved 15-bus smart-grid distribution test feeder in an OPAL RT real-time simulator.

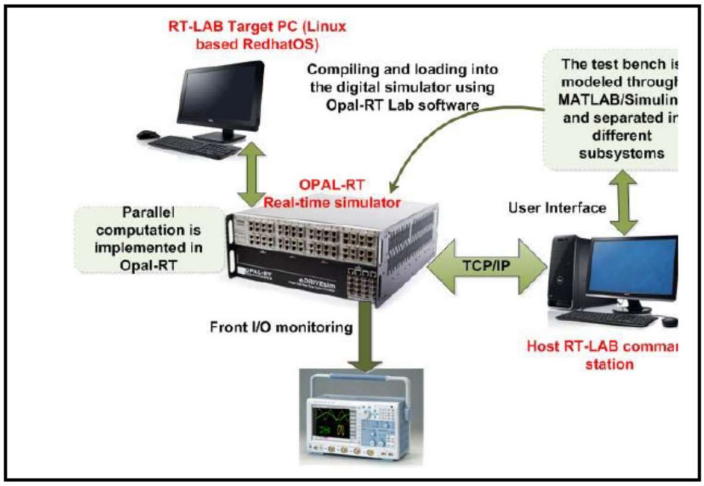

Figure 2 OPAL RT simulator system used to validate the load-shedding scheme in [29].

By using power-line communication (PLC) technology, a multi-agent based UFLS scheme was investigated [30]. This scheme used the nearest-neighbor consensus (NNCA) algorithm to detect the local power imbalance and used it to estimate the total power imbalance following the distribution of average power sharing. Then the load-shed amount was calculated and executed accordingly.

1.3 Motivation for this thesis

Power grids have started to operate around their stability limits, focusing more economic objectives for operation [2]. Moreover, upgradation of modern power system

aids to even further instability, and as a result incidents of power outage or blackout have become much more common. Blackouts have turn out to be one of the major concerns in power industries in recent years as they have an enormous socio-economic impact (e.g., Blackout in SA costed $376 million[5]). The following chart (Table-1) displays some major blackouts that happened in recent years.

Table 1 Major Blackouts around the world.

Blackout	People affected (millions)	Country	Date
South Australian blackout	1.7	Australia	28 Sep 2016
Kenya nationwide blackout	44	Kenya	07 June 2016
Sri Lanka nationwide blackout	21	Sri Lanka	13 March 2016
Turkey blackout	70	Turkey	31 March 2015
Pakistan blackout	140	Pakistan	26 January 2015
Bangladesh blackout	150	Bangladesh	1 November 2014
Blackout in India	620	India	30-31 July 2012
Paraguay and Brazil and blackout	87	Paraguay, Brazil	10-11 Nov. 2009
Blackout in Java-Bali	100	Indonesia	18 Aug. 2005
Northeast blackout	55	USA, Canada	14-15 Aug. 2003
Blackout in Italy	55	Italy, Switzerland	28 September 2003
Blackout in India	230	India	2 January 2001
Thailand nationwide blackout	40	Thailand	18 March 1978
Northeast blackout	30	USA, Canada	9 November 1965

The above table indicates that the rate of occurrence of blackouts is higher in recent times. This is an impact of recent changes in the dynamic characteristics of grid networks. Though the power system stability has been recognized as an important problem since the 1920s, recently it gets more attraction due to recent changes in the dynamic behavior of power systems. Due to the replacements of existing large generators by wind turbines, Photovoltaic units, and other renewable energy sources, the system's dynamic behavior changes significantly. Thus, the probability of losing stability and reliability of the grid network is getting higher and more unpredictable in recent times.

Frequency stability is necessary to maintain reliable operations. UFLS plays an important role to achieve frequency stability in a power system. Frequency instability

can cause generation outages leading to a blackout. Problems associated with under-frequency load shedding during a frequency-excursion process draws new attention since penetrations of renewable energy sources weaken the system's inertia. Besides, to improve a system's reliability and stability the inertia properties of renewable energy sources can be utilized, e.g. a wind turbine has synthetic inertia which can help in the frequency-excursion process, and a battery can be used as transient-time energy supporter. Considering the impacts of renewable energy sources on the grid's inertia, the probability of cascade tripping of generators has become higher due to the fast frequency response to a system disturbance. For this reason, modern grid needs regular modification in its protection scheme after assessing a system's behavior. Moreover, transient-time imbalances between generation and load consumption due to transmission line faults, generator tripping or a sudden increase of load during the UFLS process may result in a cascade tripping of generators. From the literature review mentioned above, it can be seen that the online-based UFLS schemes were not tested on a power system network that contains both synchronous machines and inertia-less renewable generators. On the other hand, offline-based predefined UFLS setting may suffer from insufficient/over curtailment of loads which degrades its performance. Therefore, it is undeniable that the existing power system needs re-modeling or adopting new method to maintain its reliability, which is the motivation of the work presented here.

Therefore, this thesis proposes an online-based UFLS scheme which is tested on a real network (a portion of Bangladesh Power Grid) that contains both synchronous generators and renewable generators. Besides, the performance of conventional UFLS schemes have been evaluated. Moreover, to compare the performance of the proposed UFLS scheme, another pre-established UFLS scheme (MILP) is tested on the test network.

1.4 Thesis Organisation and Contributions

In this thesis Chapter 2 represents a brief overview of UFLS scheme and it's components following the study of traditional UFLS schemes. Chapter 3 proposes a modified method of under frequency load shedding scheme by considering the system's damping factor in it. It also discusses how the proposed online- based modified UFLS technique overcomes the limitations of traditional UFLS methods. Chapter 4 implements the MILP program described in [6] to extract under-frequency relay parameters in both scenarios (with and without renewable penetration) to show performance comparisons between conventional, MILP, and the proposed modified on line-based UFLS scheme in Chapter 5. Chapter 6 ends with conclusions and recommendations for the future work.

Chapter 2

2.1 UFLS and Under Frequency Relay

UFLS can be described as a method applied to manage a system's load demand through shedding when its frequency drops below the normal value so that the system can be restored to a secure state avoiding blackouts. An overload condition occurs when changes take place between generation and load power: where the load increases due to a sudden collapse of generation units or due to a sudden increase of steady state load demand. During such situations, the mechanical power to the turbine through primary regulation is increased to maintain the system's frequency close to the acceptable limit as much as possible. But if the regulation limit is already reached while the overload condition is still in action, a rapid decline of frequency takes place. Overload condition can be mitigated by increasing the generations by using spinning reserves initially [7]. But in the extreme case, it may fail to protect frequency decline due to having insufficient spinning reserves. The second method is automatic load shedding based on a low frequency which is an effective technique. The device that performs automatic load shedding is under-frequency relays. Under-frequency relays are placed in every grid station where the frequency is monitored continuously. When frequency falls below any threshold limits following any overload conditions, relays execute the trip signal to the circuit breakers, which disconnect the feeders in six cycles or less (~0.1 seconds) as shown in Figure 1 [8].

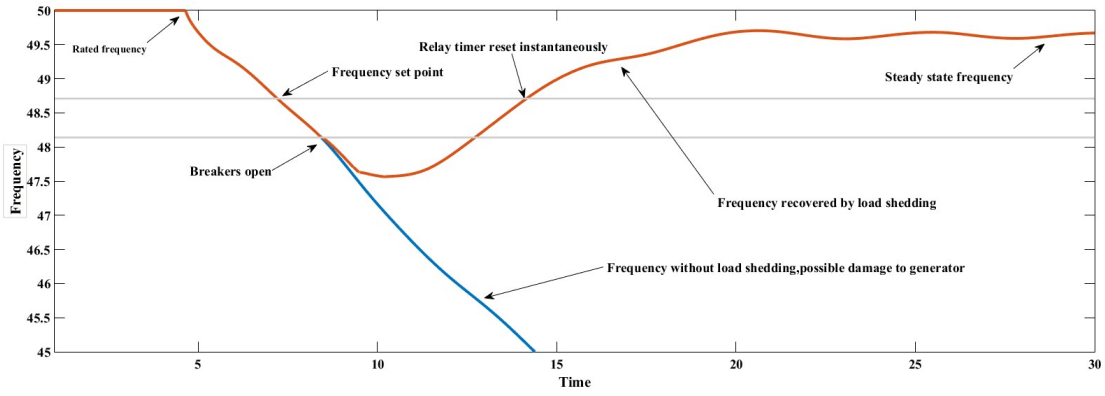

Figure 3 Simple example showing the operation of under-frequency relay actions.

Here single setpoint relay has been used to describe the function of an under-frequency relay. An under frequency relay has three parameters: (i) the frequency set point, f_s; (ii) the amount of load shed, Δd_s; and (iii) the time delay, Δt_s spent by the frequency below the set point at which load shedding occurs [9]. The logic of under frequency relay can be written as follows:

$$if\ f(t_0) = f_s\ and\ f(t) < f_s\ for\ t_0 \leq t \leq t_0 + \Delta t_s\ then\ load\ shed\ \Delta d_s$$

In this thesis, a relay that uses three set points has been used. The logic of this type of relay is:

$$if\ for\ any\ s = 1,..,3, f(t_0) = f_s\ and\ f(t) < f_s\ for\ t_0 \leq t \leq t_0 + \Delta t_s\ then\ load\ shed\ \Delta d_s$$

It is noteworthy that frequency set points must satisfy the relation: $f_s > f_{s+1}$ i.e. the frequency must fall below s before the activation of the next low level $s+1$. Tripping loads at certain frequency set points can be executed by following the rate of change of frequency like adaptive relay [10] or predefined frequency threshold limits. In addition to that, the UFLS relays also trip generating units if local frequency drops below certain critical limits for a specified time interval. For 50 Hz system the safety operating limit for the synchronous generators is 50.5-49.5 Hz [10]. Though it varies according to a manufacturer's specifications, in most cases, synchronous machines will instantly trip at 47.5 Hz. A table of typical generator off-frequency/time limit has been shown in Table-2 [10]. It is necessary for under frequency relays to maintain the frequency/time limits.

Table 2 Typical generator off-nominal frequency/time limitations.

Under frequency limit (Hz)	Over frequency limit (Hz)	Maximum permissible time
50.5-49.5	50.0-50.5	N/A(continuous operating range)
45.4-48.5	50.6-51.5	30 seconds-3 minutes
48.4-47.9	51.6-51.7	7.5 seconds
47.8-47.6		45 cycles
Less than 47.5		Instantaneous trip

2.2 Power System Dynamics

An electric power system's behavior can be described as synchronous machines behavior (Figure-2). A synchronous machine converts its mechanical power P_m, to electrical powerP_e. For synchronous operation mechanical power must be equal to electrical power i.e.

$$P_m = P_e \tag{2.1}$$

Any imbalance between this will cause instability and power system frequency starts to face a deviation from its synchronous value (e.g. for Asia, Australia etc. the synchronous frequency is 50 Hz).

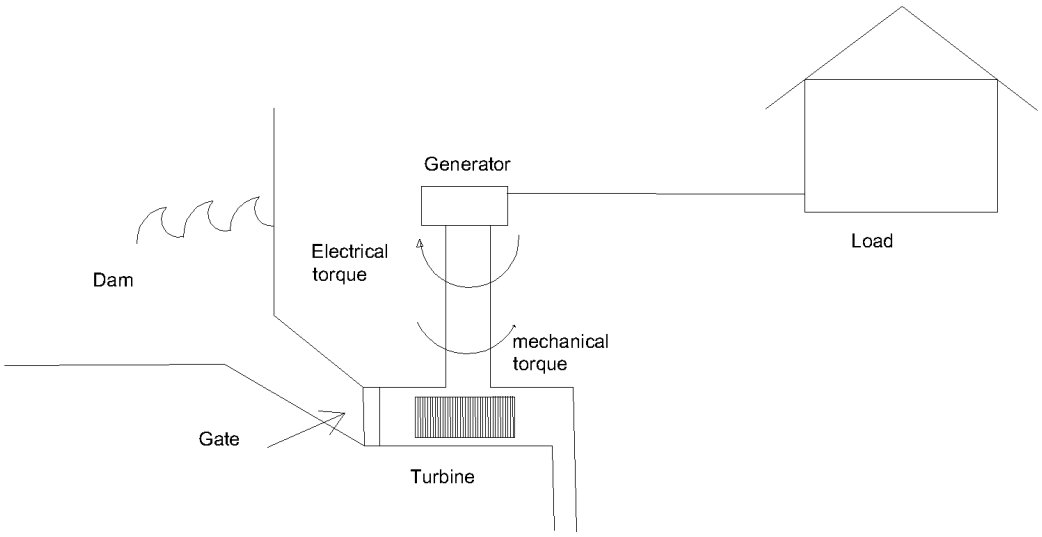

Figure 4 Simplified power system model.

The impact of imbalances between generated and consumed power on frequency can be described with the help of the swing equation [11]. For a multi-machines power system containing $i = \{1,\ldots\ldots, N\}$ generators, the swing equation for i^{th} generator is written as:

$$\frac{2H_i}{f_0}\frac{d\Delta f}{dt} = \sum P_i^{mech} - \sum P_i^{elec} \tag{2.2}$$

where H_i is the equivalent inertia of the system; f_0 is the synchronous frequency (50 Hz or 60 Hz); Δf frequency deviation of power system which is zero under balance condition; and $\sum P_i^{mech}$, $\sum P_i^{elec}$ are equivalent mechanical and electrical power. When any of the i^{th} generator trips, the power imbalance between the electrical and mechanical power creates accelerations in frequency deviation Δf from steady state. This deviation depends on a system's equivalent inertia, load damping factor, amount of power imbalance etc. Figure 3 shows the impact of frequency deviations due to overload conditions.

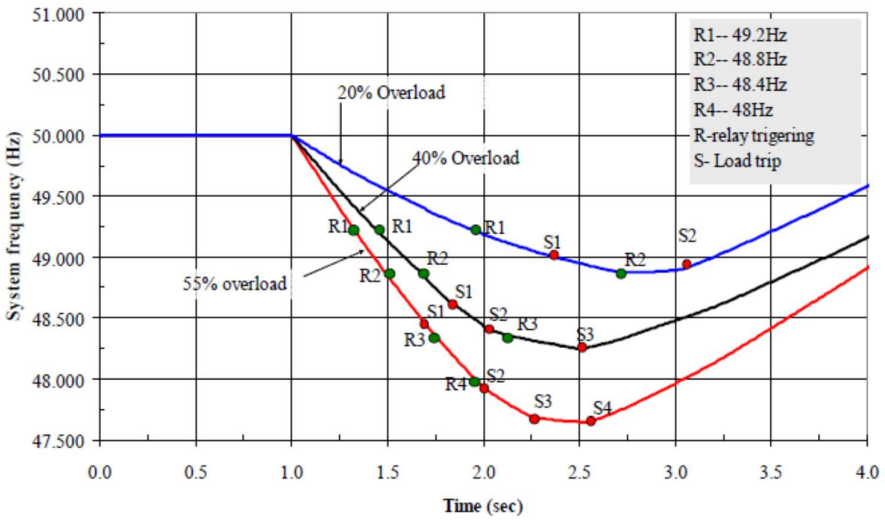

Figure 5 Characteristic of the system frequency- response due to overloads [12].

2.3 Frequency-dependence of Loads

Power System contains various loads including resistive, inductive and capacitive loads. Resistive loads such as incandescent lights, resistors, heaters etc. are independent of frequency. But the inductive load like motors have an impact of frequency dependency. Load frequency dependency have an impact on active power consumption which can be formulated as:

$$\Delta P_{active} = D\Delta f \tag{2.3}$$

where D is the damping factor (typical value of which is 2%), ΔP_{active} is the change in active power and Δf is the change in frequency deviation. Due to a sudden change in frequency, the active power consumption reduces. Figure4 shows the impact of load damping considering 50% generation loss. By considering the load-frequency dependency, the swing equation can be modified as:

$$\frac{2H_i}{f_0}\frac{d\Delta f}{dt} = \sum P_i^{mech} - \sum P_i^{elec} - D\Delta f \tag{2.4}$$

Though the impact of damping on frequency decline has less impact (2% only) but authors in [10] indicated that it has a great impact on load shedding. By considering this damping impact, the under frequency load shedding can be accurately determined.

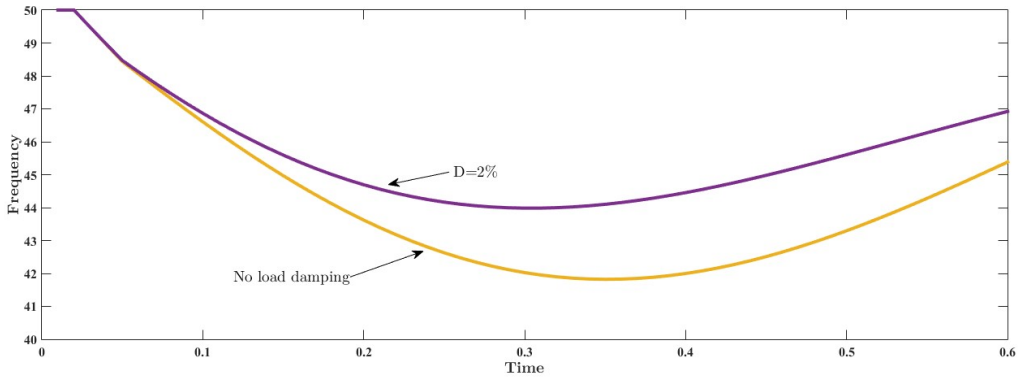

Figure 6 Effect of frequency-dependence of loads due to a 50% generation loss.

2.4 Primary frequency regulations through governor action

The automatic change in active power generation of generating units following a change in a system's frequency is called primary frequency regulation [7]. After any loss of generating units in an interconnected system, the system frequency decreases from its nominal value as the kinetic energy of the rotating masses decreases. Each generating unit i located in synchronous zone with frequency deviation Δf is fitted with speed governors that automatically respond to such a deviation by incrementing its active power generation by $-\frac{\Delta f}{R_i}$, subject to capacity and ramp limits (Figure 5). Here parameter R_i denotes frequency regulation constant or governor droop of unit i in Hz/MW; typical values of governor droop lies between 4 and 6 Hz for the loss of rated power.

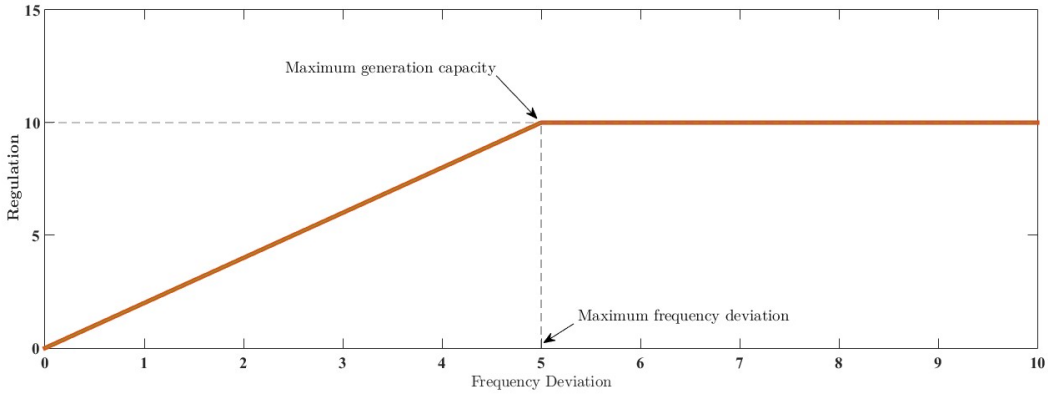

Figure 7 Primary frequency regulation characteristics of unit i [13].

2.5 Discrete-Time Frequency Response Model

In a multi machine power system with $i = \{1, \ldots\ldots, N\}$ generators, depending on governor droop, inertia constant etc. each generator has a unique frequency response to a contingency. However, for a synchronous system, frequency response can be

considered as equivalent of a single-machine swing response. In time domain the swing equation can be written as:

$$\frac{d\Delta f(t)}{dt} = \frac{f_0}{2H}(\Delta r(t) - \Delta g + \Delta d(t) - D\Delta f(t) \tag{2.5}$$

where $\Delta f(t)$ is the frequency deviation from nominal value at time t following a generation loss Δg at $t = 0$. Δr denotes the governor droop at time t and D is the total damping factor. The relation between primary frequency regulation r and droop time constant T can be expressed by:

$$\frac{d\Delta r(t)}{dt} = \frac{1}{T}(-\Delta r(t) - \frac{\Delta f(t)}{R}) \tag{2.6}$$

In equation (1.5) the equivalent inertia can be expressed by,

$$H = \sum_i \frac{H_i S_i}{S} \tag{2.7}$$

where S is the system power base while S_i is individual power base of generators. In addition, governor droop R in equation (1.6) can be calculated as:

$$\frac{1}{R} = \sum_i \frac{H_i S_i}{S} \tag{2.8}$$

However, for simulation purpose equation (1.5) and equation (1.6) need to be discretised into time step Δt by defining $\Delta r(n\Delta t) = \Delta r_n$, $\Delta d(n\Delta t) = \Delta d_n$, and $\Delta f(n\Delta t) = \Delta f_n$. Then through Euler's method, equation (1.6) in discrete form becomes,

$$\Delta f_n = \Delta f_{n-1} + K_{n-1}\Delta t; \quad \forall\, n \tag{2.9}$$

where K_{n-1} is frequency gradient which can be expressed by:

$$K_n = \frac{f_0}{2H}(\Delta r_n - \Delta g + \Delta d_n - D\Delta f_n) \tag{2.10}$$

While equation (1.6) takes the following form in discrete model

$$\Delta r_n = \Delta r_{n-1} + \frac{\Delta t}{T}(-\frac{\Delta f_n}{R} - \Delta r_{n-1}) \tag{2.11}$$

The initial value of Δf_{n-1} and Δr_{n-1} are equivalent to zero since prior to the contingency there is no frequency deviation and primary frequency regulation. Time steps Δt is an important factor in terms of simulation accuracy (see Figure 6). Smaller time steps provide higher accuracy. It is important to use enough time steps so that frequency can reach in steady-state condition typically within 20 sec.

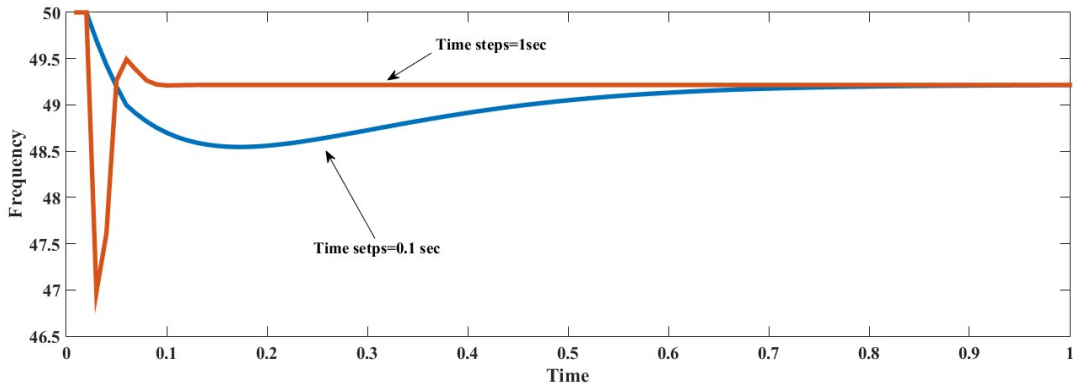

Figure 8 Impact of time steps.

2.6 Impact of System Inertia on Frequency Response

The inertia of a Power system containing multi-machines depends on individual machines' inertia. When a synchronous machine is replaced with any renewable energy sources (e.g. Wind Plant, Solar Plant etc.), the system's inertia becomes weaker since with this replacement, the contribution of one synchronous machines' inertia is lost. Equation (1.9) and (1.1.0) clearly depict the impact of inertia on frequency deviations. From equation (1.10), it is clear that frequency gradient is inversely proportion to the system's inertia In modern power grid renewable sources are being connected through inverters which has no inertia. So, by replacing a synchronous generator a system's strength is reduced. Weaker strength of a modern power system causes more frequency deviation to any contingency (see Figure 6).

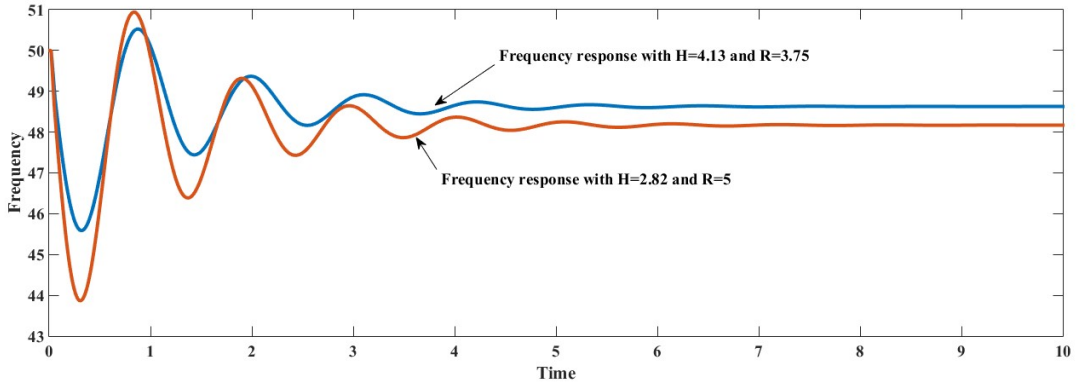

Figure 9 Impact of inertia on system frequency response following 50% generation loss.

It is noteworthy that here the impact of inertia has been shown using matlab simulation by using the test network data and considering random (not optimised) under-frequency load shedding. More details is provided later.

The following section discusses the study of the conventional under frequency load shedding plan. The steps of conventional UFLS scheme are taken from [31] and [32]. The conventional scheme are implied on a real test network described below. Then, the impact of renewable energy penetrations on the conventional settings are discussed in detail.

2.7 Conventional under frequency Load shedding Methodology

The steps of conventional UFLS schemes is discussed below-

Step 1: Selection of the highest overload condition for which a load shedding program is to set to protect the frequency decline and bring it to steady state within the acceptable limits.

Regardless of the design method, the first step is to determine the maximum overload condition for which the setting will provide coverage. This overload conditions varies from region to region or country to country. For example according to [33], UFLS plans in North America considered maximum overload conditions between 25% to 70%. Again in [6] the maximum overload condition was considered 50% of generation loss. In this research 50% of generation losses are used as highest overload conditions. In addition to that for steady state a frequency deviation of 0.5 Hz on 50Hz frequency is considered[6].

Step 2: Determination of total required load to be shed.

Calculation of total amount of load shedding is estimated by the following equation[31]:

$$\Delta d_T = \frac{\frac{L}{1+L} - d(1-\frac{f}{50})}{1 - d(1-\frac{f}{50})} \tag{2.12}$$

where Δd_T refers to total load shedding amount, d indicates the load damping factor, and L is the per unit system overload, which is the ratio of generation loss to total remaining generations. Equation (3.41) will give us the conservative load shedding amount. To calculate the load shedding amount, the following values are considered.

For per unit system overload $L = 1$ (50% of generation losses), total load damping factor, $d = 2$ (2% damping, i.e. 2% load reduction per 1% of frequency reduction), steady state settling frequency is considered $as\ f = 40.5\ Hz$. Then the total amount of load shedding is calculated as:

$$\Delta d_T = \frac{\frac{1}{1+1} - 2(1-\frac{49.5}{50})}{1 - 2(1-\frac{49.5}{50})} = 0.489 \approx 0.49 \tag{2.13}$$

Therefore, the UFLS plan must be designed to shed total load of 0.49 per unit.

Step 3: Selection of number of stages and load shedding amount per stages

According to [34] and [31] load shedding stage can be lied between 3 to 5 stages for optimum load shedding per stage. But the choice is arbitrary. In this thesis, a three stage under frequency relay user model "LDSHBL" [35] in PSS/E are used. After selecting the number of stages, it is important to select the per stage load shedding amounts. It is preferable to shed less in the primary stages and increase the amount of load shedding in the following stages [36]. In this way for small contingency unnecessary load shedding can be avoided. For the test system described below the total amount of load shedding, which is calculated above are divided into three blocks (0.14, 0.16, and 0.19 pu) by considering a trial setting. Once t the value of each stage load shedding amount is achieved, the three stage frequency set points need to be determined.

Step 4: Determination of relay frequency set points

The main objective of this step is to determine frequency set points. Though this choice is arbitrary but based on some general rules combined with knowledge of the system this choice can be made accurately. In [31],[32] and [34] it is suggested that load shedding at highest possible setting point should be executed since early stage load shedding limits the maximum frequency deviation. However, to avoid load shedding at mild contingency it is recommended that first frequency set point should be not higher that the maximum allowed frequency deviation level (i.e. 49.5 Hz). Therefore, the first frequency set point is chosen at 49.4 Hz. The lowest frequency set point should be above the minimum allowed frequency to avoid the tripping of generators. Although it varies according to manufacturer's specifications, in most cases, synchronous machines will instantly trip at 47.5 Hz. Therefore, the frequency excursion process should not allow the frequency below that level to avoid the synchronous generators to trip, which might lead to possible blackouts. So, in this thesis the last set point is considered above 47.5 Hz. By considering relay time delay and by considering an error margin of 0.2Hz, the lowest frequency set point is considered at 47.9 Hz. Now to select the middle set point step 3 is being followed. Here a trial frequency threshold is selected and the scheme is tested. If the setting is not successful then there is an iteration of steps 3 and 4 until a suitable strategy is found [6]. For trial UFLS plan, the second frequency set point is selected at 48.6 Hz. Thus, the three set points became as shown in the following Table.

Frequency (Hz)	Load shed (in P.U)	Time (Sec)
49.4	0.14	0.2
48.6	0.16	0.2
47.9	0.19	0.2

Then the setting is tested in the test network by Python based PSS/E simulation.

2.8 Test Network

In this thesis, a small portion from the Bangladesh power network is considered to implement the conventional and proposed UFLS scheme (Shown in Figure 13). This system consists of 7 synchronous generators (G1-G7) and 5 loads. The detail parameter of the system can be found in [37]. The single line diagram is shown in Figure 10**.** The total load on the system is, P_L=434.46 MW and Q_L=149 MVAR and the total generations capacity is, P_G= 590 MW. Transformer and the transmission lines is included in the reduced admittance matrix [38]. The generators are equipped with slow excitation system (IEEE-DC 1A) [39]and the loads are considered as static loads. In order to perform dynamic simulations and according to the recommendation of [40], constant current and constant impedance models are considered for the active and reactive components of static load modelling. Generators G1, G4, and G6 are replaced by constant power solar model to perform the dynamic simulations in the presence of renewable energy. The electrical models of the PV system with their associated control systems in PSS/E are briefly introduced [41]. The details of the solar model is shown below[40]:

- PVGU: Power converter/generator module
- PVEU: Electrical control module
- PANEL: Linearized model of a panel's output curve
- IRRAD: Linearized solar irradiance profile

Appendix A shows the PV system dynamic model in PSS/E to simulate the performance of a PV plant connected to the grid through a power electronics-based conversion system. The IRRAD module provides the capability to input an irradiance profile including up to ten (10) data points in terms of time and irradiance values[41]. At each simulation step, the module will calculate the linearized irradiance value. Then the irradiance value is fed to the PANEL module which calculates the DC power from the PV plant at the corresponding irradiance level based on I-V curves from PV manufactures. The converter module (PVGU) calculates the current injection to the

grid based on filtered active and reactive power commands from the electrical control module (PVEU). Both components of the injected current are processed under the high/low voltage conditions by means of the specific logic diagram as shown in Figure 11 in (Appendix A), which is re-produced and revised from [42].The core component in the converter based conversion system is the associated control system. In PSS/E, the electrical control module for the PV generation system (PVEU) is shown in Appendix-A. The control system consists of decoupled active and reactive power control logics to achieve different regulation objectives. The dynamic data sheet of the above modules which are used for grid connected PV module are also provided in appendix-A [43].

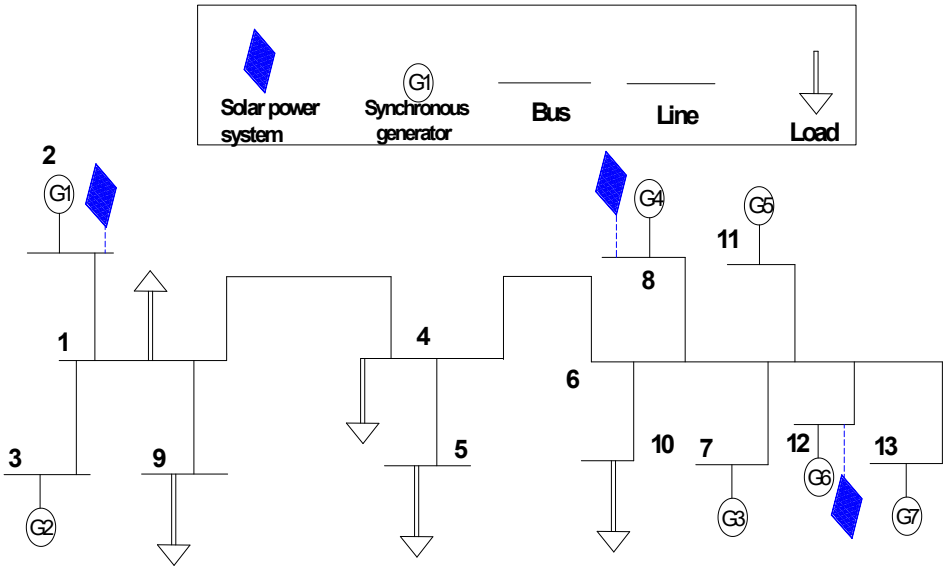

Figure 10 Test Network.

At first, the performance of the test network is analysed with no renewable penetrations to verify the function of conventional UFLS settings. In this circumstance, G1-G7 all are synchronous generators for which the conventional UFLS scheme is tested. Then, renewable energy (constant power solar model described above) replaced G1, G4 and G6 synchronous generators (shown in Figure 13) to verify the efficacy of conventional settings with renewable injections.

2.9 Conventional UFLS Setting

In this section the conventional UFLS scheme is implemented on the test network. The settings follow the rule described in Section 3.1. In this case the load shed amount is set out by considering the worst contingency condition or 50% of generation outage. According to IEEE guidelines for UFLS, load shedding can be carried out in 3 to 5 stages. By using the test network's dynamic properties, the amount of load sheds in each stage are calculated and

distributed by following equation (3.2). In addition to that, test network is considered in several contingencies. The dynamic properties of a network can be different with each contingency. The value of a system's inertia and governor equivalent droop are estimated (Shown in Table 3). These parameters are being used by the following methods.

Table 3 Contingencies with related inertia and governor droop constants.

Contingency	Generation loss (%)	Loss units	Equivalent Inertia H_{eq} (Sec)	Equivalent governor droop R_{eq} (Hz/442 MW)
1	8	G3	1.3893	4.8468
2	20	G2 & G3	1.1564	7.071
3	44	G7	1.0663	6.6362
4	8	G1	1.806	4.0111
5	20	G2 & G4	1.573	5.4172

In order to avoid more load shedding in the middle of contingencies, the total amount of load shedding is distributed into three blocks in which smaller blocks are kept in the primary stages. The above process is used to set the conventional UFLS parameters and the summary of the settings are given in Table 4

Table 4 Conventional settings for under frequency relay.

Frequency (Hz)	**Load shed (in P.U)**	**Time (Sec)**
49.4	0.14	0.2
48.6	0.16	0.2
47.9	0.19	0.2

The frequency excursion with the conventional settings without any renewable penetration is shown in Figure 14. For simplicity only three contingencies from Table 3 are considered.

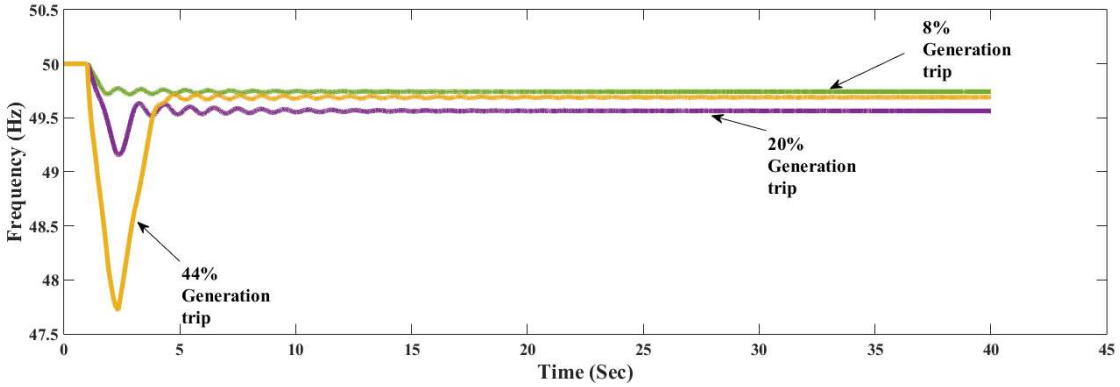

Figure 11 Frequency responses before renewable energy penetration with conventional setting.

The figure clearly depicts that with conventional UFLS setting, the test network survived frequency excursion below the threshold limits (47.5 Hz) in any contingencies.

2.10 Impact of Renewables energy on the performance of conventional UFLS scheme

In the previous section, it was shown that traditional UFLS settings work fine with no renewable penetrations. However, with the integration of 27% of renewable energy sources (G1, G4 and G6 synchronous generators, are replaced with the constant power PV module as in Figure 13) the conventional load shedding scheme exhibits the following frequency responses for the same contingencies shown in the Figure 15.

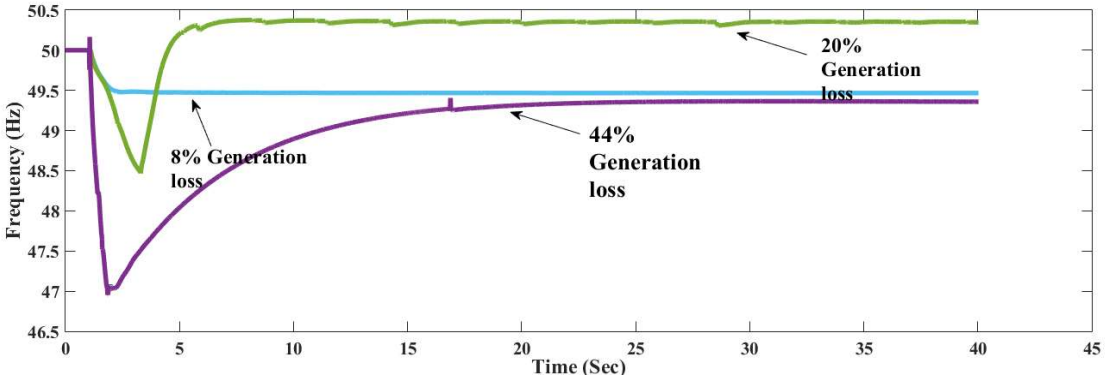

Figure 12 Frequency responses after 27% renewable energy (Solar energy) penetration with conventional setting.

From the above figure it is clear that although the traditional UFLS settings work for 8% and 20% generation loss but with the worst contingency (44% generation tripping), it fails to protect the frequency decline within the thresholds (47.5 Hz). Below this limits all remaining generators will trip instantly and the consequence leads to

blackouts. It is noticeable that this time the amount of under frequency load shedding was greater than the previous case study.

To show the impact of renewable energy integrations to a grid network, a comparison on UFLS performance with different amount of renewable penetrations is conducted here.

Table 5 27% of Solar Energy Penetrations (From Load Flow data).

Generator	**Machines**	**Active power generation**	**Reactive power generation**	**Worst Contingency**
G1	SOLAR 11.000	53.4	39	G7 is disconnected at Time T=1sec creating 44% contingency (worst one)
G2	JAM_2 11.000	53.4	39	
G3	RPCL 150 11.000	35	23.1	
G4	SOLAR 11.000	35	23.1	
G5	TERMINAL 11.000	35	23.1	
G6	SOLAR 11.000	35	23.1	
G7	TERMINAL(2) 10.500	195.2	72.1	
Total generation		442	242.5	

Table 6 16% of Solar Energy Penetrations (From Load Flow data).

Generator	**Machines**	**Active power generation**	**Reactive power generation**	**Worst Contingency**
G1	JAM_1 11.000	53.4	39	G7 is disconnected at Time T=1sec creating 44% contingency (worst one)
G2	JAM_2 11.000	53.4	39	
G3	RPCL 150 11.000	35	23.1	
G4	RPCL 210 11.000	35	23.1	
G5	SOLAR 11.000	35	23.1	
G6	SOLAR 11.000	35	23.1	
G7	TERMINAL(2) 10.500	195.2	72.1	
Total generation		442	242.5	

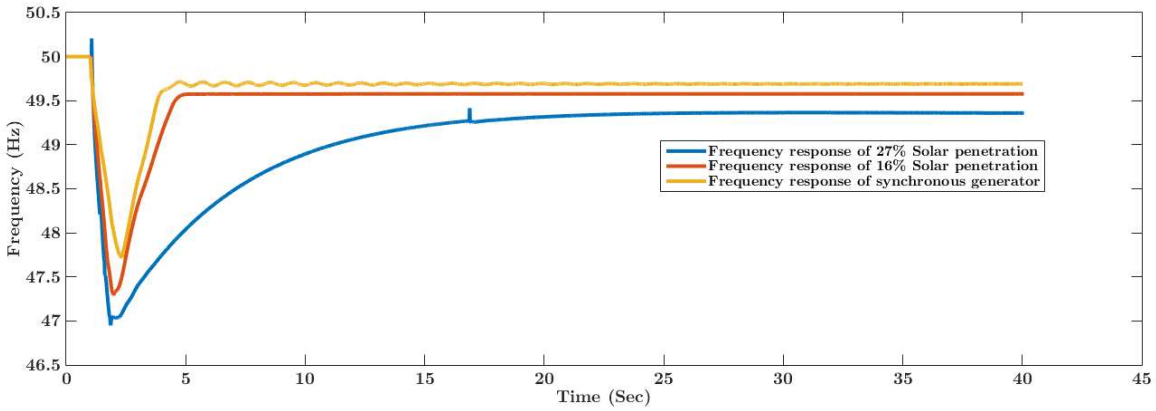

Figure 13 Frequency responses of different amount of Solar Energy Penetrations following worst contingency (44% Gen loss) with traditional UFLS scheme.

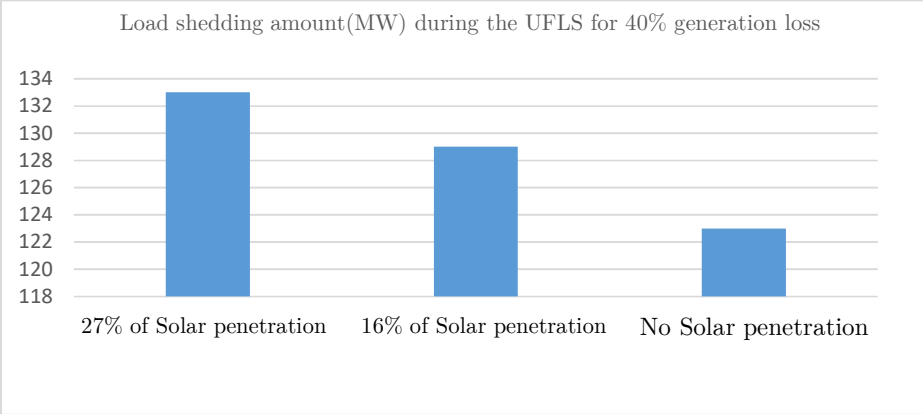

Figure 14 Impact of renewable interference on the amount of load-shedding to limit frequency excursion.

From Figures 16 and 17, it can be concluded that before Solar energy penetrations conventional scheme succeeded to restrict frequency decline within the safe limits but with the replacement of two synchronous generators with the converter connected solar system, the system starts to face problem to restrict frequency decline within the safe limits. This leads the system to lose remaining generation at once. In addition to that, with the increment of solar penetrations the amount of load shedding increases. Conventional way of frequency excursion process is proving insufficient to maintain the stability of a low inertia based power system, which is one of the major reasons for modern grid blackouts.

2.11 Limitations of Traditional UFLS schemes

Although the conventional settings can restrict frequency decline successfully with a high system's strength but it gets weaker due to the injection of renewable sources,

resulting in a noticeable degradation on the performance of the conventional one. Many utilities including AEMO, Australia have started to revise their UFLS settings every 6/12 months to remodel the protection system according to the new system strength. In addition to that, any pre-set load curtailment strategy may fail to achieve the frequency excursion due to the uncertain nature of dynamic loads. Chapter 3 proposes a modified on-line based UFLS method to overcome the limitations of traditional UFLS schemes.

Chapter 3

3.1 Introduction

In this chapter, an online based modified under frequency load shedding method is presented. Firstly, the modelling of the proposed system is illustrated. Then, the method is implemented on the test network to verify its effectiveness. Like chapter 2, three cases are studied in this chapter with the proposed method. The effectiveness of the proposed UFLS scheme is verified using the Python-based PSS/E simulator followed by a comparison study with the traditional UFLS scheme.

3.2 Modelling of the proposed system

The UFLS scheme proposed in this case is designed by utilizing the formulation of the swing equation. To design a load shedding scheme properly, the amount of shortage of power or the power deficit is required to be measured. The amount of power deficiency can be measured in two different ways. In one method the status of the breaker near to generator is monitored and if the breaker is open, the most recent power output of that generator can be used as power shortage amount. The other method is on the calculation of the power deficit amount by using the swing equation[44]. In a renewable-source-connected grid system, the power shortage may be occurred due to various reasons, such as sudden loss of synchronous machines, lack of wind power, lack of sunlight etc. In this thesis, the second method is considered to measure the amount of deficiency of the power output. To decide the load shedding amount, the center-of-inertia frequency is calculated as [44]:

$$f_{COI} = \frac{\sum_{i=1}^{N} H_i f_i}{\sum_{i=1}^{N} H_i} \tag{3.1}$$

where,

N is the number of connected generators;

H_i is the inertia constant of each generator in seconds, and

f_i is the frequency of each generator in Hertz.

The minimization of the load shedding amount can be achieved by utilizing the total spinning reserve of the system which is dependent on the capacity of the generator. The following equation can be used to determine the total spinning reserve:

$$TSR = \sum_{i=1}^{N} MGC_i - \sum_{i=1}^{N} AGP_i \tag{3.2}$$

where

$N =$ The number of the connected generators,

$MGC_i =$ The maximum capacity of the i-th generator,

and $AGP_i =$ The actual generated power of the i-th generator. Then power deficit amount can be calculated by:

$$P_{deficit} = \frac{2\times\left|{}^{df_{COI}}/_{dt}\right|\times H_{eq}}{f_n} \tag{3.3}$$

where $P_{deficit}$ is the power deficit; ${}^{df_{COI}}/_{dt}$ is the rate of change in center-of-inertia frequency deviation; f_n is the nominal frequency which is 50 Hz in our case, and finally H_{eq} is calculated as:

$$\mathrm{H_{eq}} = \sum_{\mathrm{i}} \frac{\mathrm{H_i S_i}}{\mathrm{S}} \tag{3.4}$$

In another way, the deficiency of the output power can be estimated by using the information of disconnected sources as:

$$P_{deficit} = \sum_{j=1}^{N} P_{\ disconnected\ source} \tag{3.5}$$

where $P_{deficit}$ is the power imbalance and N is the number of disconnected sources and $P_{\ disconnected\ sourc}$ is the disconnected power from the generators. Then actual amount of load shedding can be evaluated as:

$$TLSA = P_{deficit} - TSR \tag{3.6}$$

The primary frequency control can be started at a frequency level of 49.8 Hz [45]. But it can be varied depending on the level of protection needed. In Bangladesh, the lack of spinning reserve was one of the main reasons for the September 2014 blackouts. Therefore, the spinning reserve is considered as zero in the proposed load-shedding scheme (i.e.$TSR = 0$). The impact of load damping (D) is also considered, which can reduce the load shedding amount. When an imbalance of power occurs due to disturbance, the amount of power deficiency is calculated from equation (3). Since the zero spinning reserve is considered in this work, so the total load shedding amount would be equal to the power deficit following (6). However, in the proposed UFLS scheme, the system's total damping impact is considered, and will be calculated by the following equation[33]:

$$\beta = D + \frac{1}{R_{eq}} \tag{3.7}$$

where β the total damping is factor; D is the load-frequency sensitivity factor (value 2 is considered here); and R_{eq} is the equivalent speed governor droop which can be calculated as:

$$\frac{1}{R_{eq}} = \sum_i \frac{1}{R_i} \tag{3.8}$$

where $R_{i\ is}$ the speed droop constant of i generators. In the proposed load shedding method, the maximum allowable frequency deviation is considered as ±0.5 Hz. By taking this limit into consideration, the formula to determine the total amount of load shedding can be revised. Therefore, the total allowable power deficit amount can be calculated as:

$$\Delta P_{max} = \beta \times \Delta f_{ss} \tag{3.9}$$

where $\Delta f_{ss} = \frac{maximum\ allowable\ frequency\ deviation\ (0.5\ Hz)}{Nominal\ frequency(50\ Hz\ for\ our\ system)}$; ΔP_{max} is the amount of maximum allowable power deficit; β is the total system damping factor. Now the total amount of load shedding will be:

$$TLSA = P_{deficit} - \Delta P_{max} \tag{3.10}$$

After any imbalance of power or any disturbance in the power grid, the power deficit amount is calculated by using equation (4.3). By considering the total system's damping factor, the necessary load shedding amount is calculated and distributed in each of the 3 stages according to [46]. It is worth mention that, by taking the total system's damping factor into account the amount of actual load shed can be minimized.

3.3 Case studies

The proposed UFLS scheme re-assessed the amount of load shedding and the traditional scheme is redesigned. The following cases are considered in order to analyse the impacts of the proposed load shedding scheme on the frequency excursion process and to observe the scheme's performance.

Case-1: Outage of 44% of generations in an islanded network

In this case study, the highest possible generation losses (the worst case scenario) are considered. The conventional load shedding scheme failed to arrest frequency within the threshold limit (47.5 Hz) in the presence of renewable energy sources as shown in Figure 15. This case study is performed to investigate whether the proposed load shedding can successfully arrest frequency excursion within the threshold limit or not. In this case, the test network is modeled with 27% of solar energy sources as a constant power model (as described in Section 3.2. After the load flow study, the frequency responses following a generation loss (44% of total generation) at bus-13 is considered. In order to distribute the amount of load shedding, the procedure described in [44] is taken into account. In this process, the frequency deviations and the amount of load to be shed is calculated through the microprocessor-based-controller (which needs to be programmed). The controller sends the load shedding signals to the relay according to load priorities to disconnect the load. It is assumed that load shedding will be

controlled from one end, and the relay pickup time (including the CB tripping time) is around 200 ms [44].

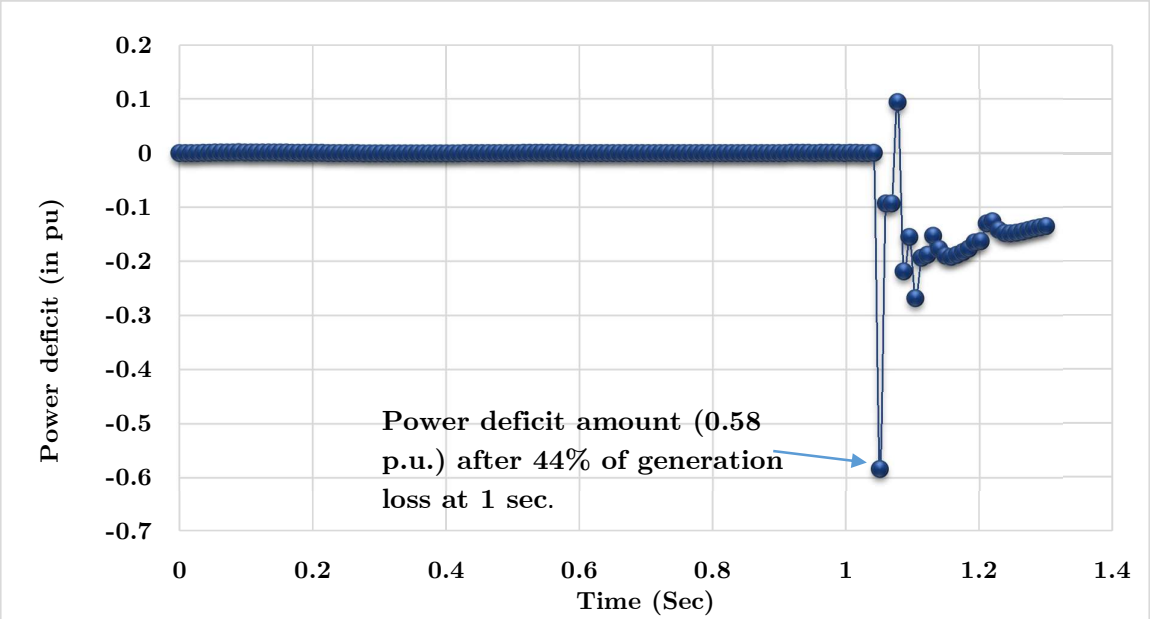

Figure 15 Power deficits in the moment of 44% of generation loss.

Figure 18 shows the amount of power shortage due to 44% generation loss. It shows only a few seconds of data to show the impact of generation loss in terms of power deficit amount. By using the equations from (4.7) to (4.10) the amount of total load shedding needed is calculated by considering the system damping factor (D) as 2%, and using the equivalent governor droop (R_{eq}) of the remaining generators. From the calculation,

$$\beta = 9.53$$

$$\Delta P_{max} = \beta \times \Delta f_{ss} = 9.53 \times \frac{0.5}{50} = 0.0953$$

$$TLSA = 0.58\text{-}\ \Delta P_{max} = 0.58 - 0.0953 = 0.4846\, pu$$

It is noteworthy mentioning that the maximum steady state frequency deviations is allowed up to 0.5 Hz from the nominal value (50 Hz). This value can be used as user-defined data, i.e. if it is required that steady-state frequency deviations should not exceed 0.4, 0.3 or 0.2 Hz from the nominal value, load shedding amount will be changed with those requirements. In this case maximum steady state frequency deviation is considered to reduce the amount of load shedding. Then, the load shedding amounts are divided into three stages following the guidelines (45% in the first stage, 35% in the second stage and 20% in the third stage) in [44].

The modified UFLS settings and frequency response are shown in Table 7 and Figure 19.

Table 7 Proposed settings for under-frequency relay for 44% of generation loss.

Frequency (Hz)	Load shed (in P.U)	Time (Sec)
49.4	0.21	0.2
48.6	0.17	0.2
47.9	0.09	0.2

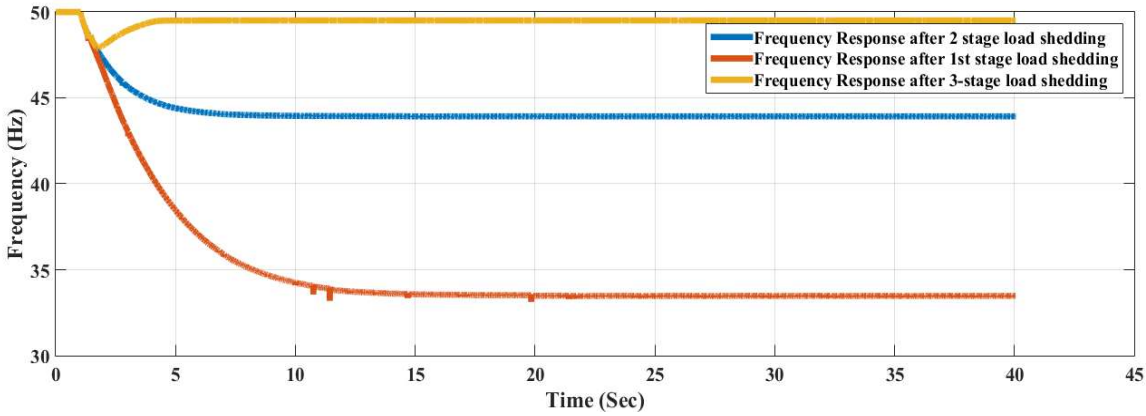

Figure 16 Frequency responses of different stages of load shedding after 27% renewable energy (Solar energy) penetration with the proposed setting for 1st contingency.

Moreover, a graphical presentation of the rate of change of frequency is presented with respect to the frequency in Figure 19. From the figure, it can be seen that for 44% of generation loss frequency recovers within the threshold limits (47.5 Hz) and the ROCOF tends to zero at the pre-set steady-state value (49.5 Hz). Therefore, this study successfully satisfies the process of frequency excursion process within the acceptable threshold limits which will prevent further loss of generations due to under-frequency tripping.

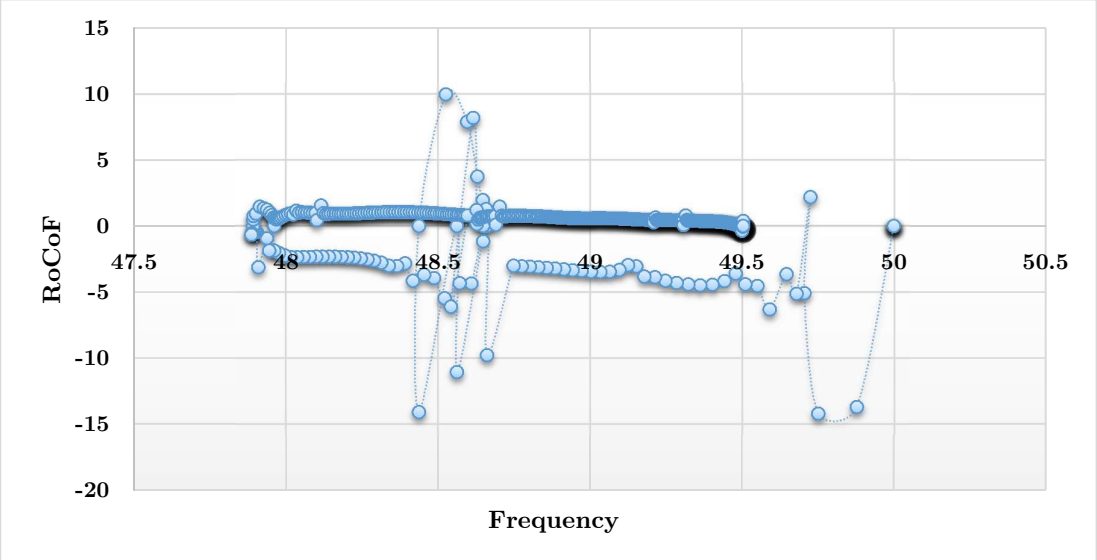

Figure 17 Relation between RoCoF vs. Frequency for Case 1.

Case-2: Outage of 20% of generations in an islanded network

The performance of the proposed load shedding scheme is tested for another scenario (20% of generation outage). In this scenario, the generators from bus -3 and bus-7 are disconnected and the performance is evaluated. The power deficit amount is shown in the following Figure.

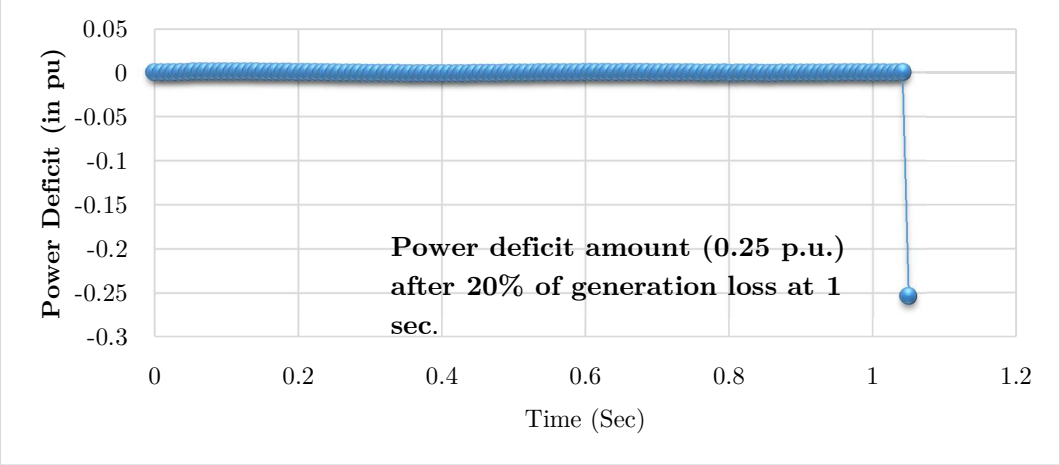

Figure 18 Power deficits in the moment of 44% of generation loss.

Calculations in case study 1 are repeated here to extract the amount of load shedding and then it is divided into three stages. The modified UFLS settings and the frequency responses are shown in Table 8 and Figure 22.

Table 8 Proposed settings for under-frequency relay for 20% of generation loss.

Frequency (Hz)	Load shed (in P.U)	Time (Sec)
49.4	0.07	0.2
48.6	0.05	0.2
47.9	0.03	0.2

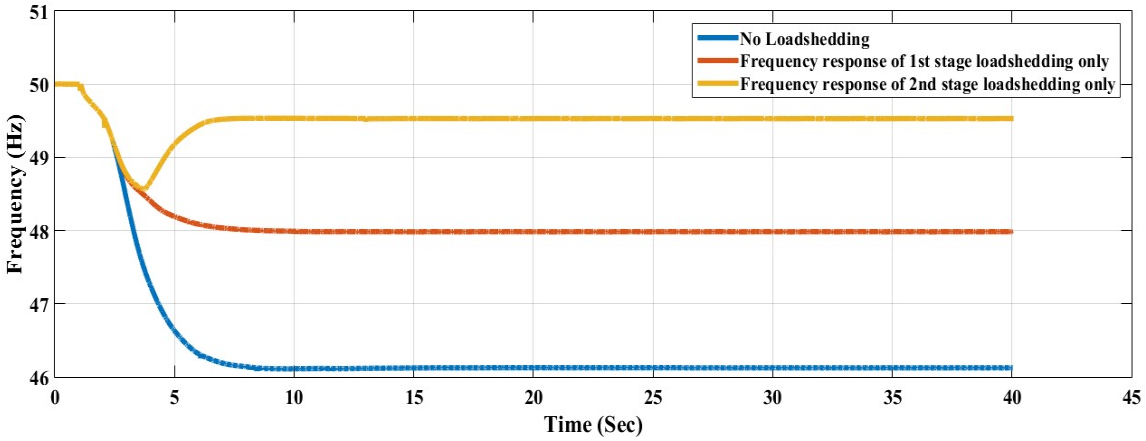

Figure 19 Frequency responses of different stages of load shedding after 27% renewable energy (Solar energy) penetration with the proposed setting for 2nd contingency.

Like Figure 19, Figure 21 also describes that the proposed method of UFLS scheme successfully restricts frequency decline within the acceptable limits.

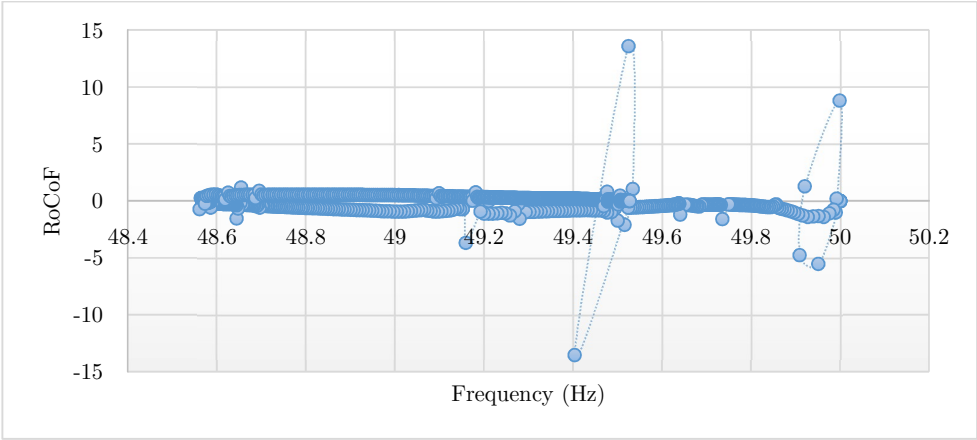

Figure 20 Relation between RoCoF vs. Frequency for Case 2.

Case-3: Outage of 8% of generations in an islanded network

In this case study, no load shedding is required by the proposed UFLS scheme at all as the frequency deviations are within the maximum limit due to the lowest contingency. Fig. 6 shows the frequency response due to 8% of generation loss

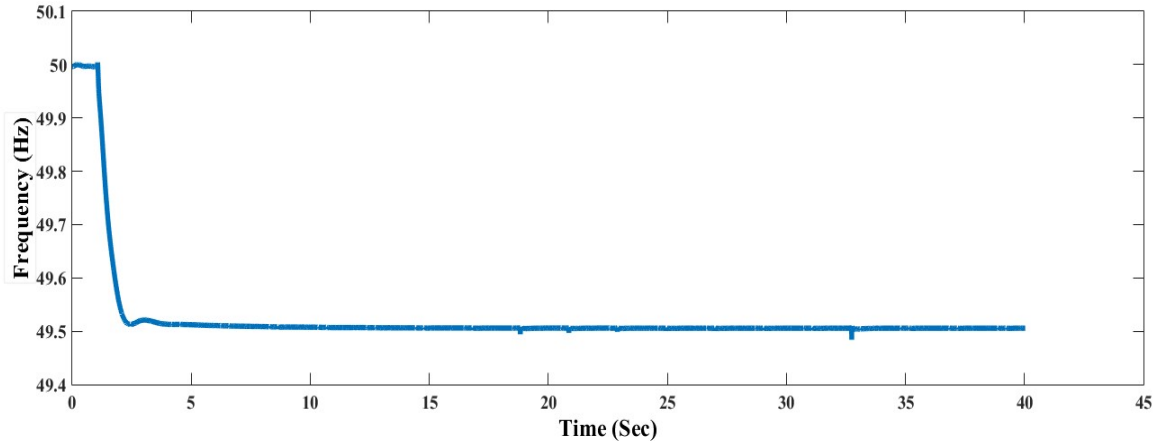

Figure 21 Frequency responses of different stages of load shedding after 27% renewable energy (Solar energy) penetration with the proposed setting for 3rd contingency.

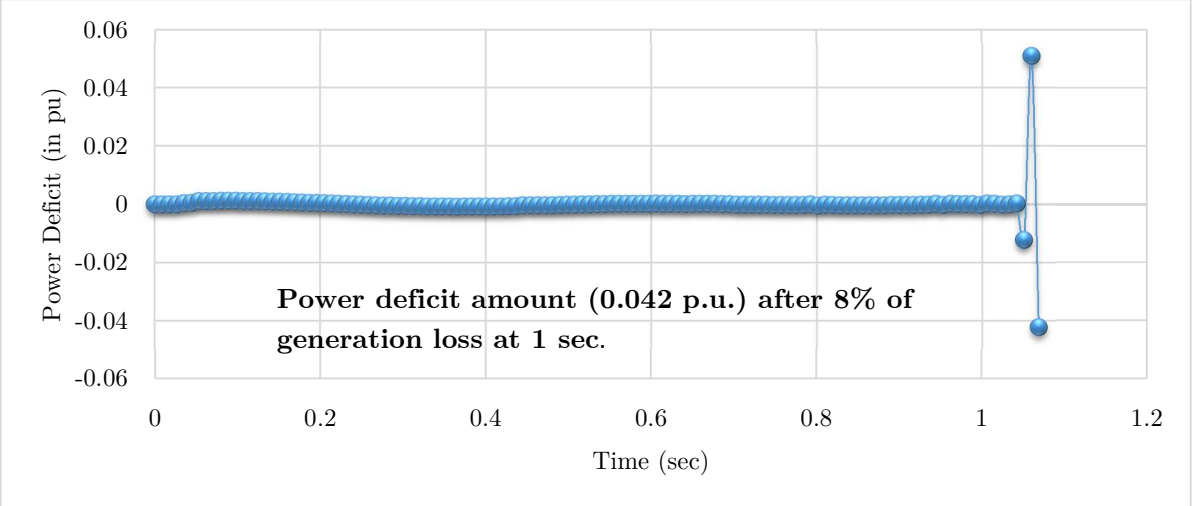

Figure 22 Power deficits in the moment of 8% of generation loss.

Figure 25 shows the shortage amount of power (0.0421 p.u.) is less than the maximum allowable power deficits (0.0953 p.u.). Hence the decline of frequency doesn't go below the first frequency threshold limit (see Figure 26), and the 3rd contingency (8% of generation loss) doesn't need any load shed.

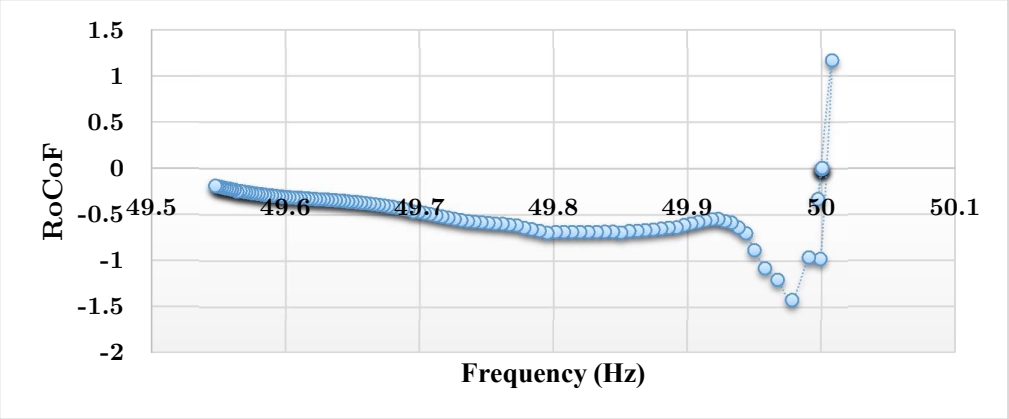

Figure 23 Relation between RoCoF vs. Frequency for Case 3.

3.4 Comparisons of the Proposed UFLS scheme with the traditional scheme

The safety operating limit for the synchronous generators is 50.5-49.5 Hz (50 Hz power system)[47]. Although it varies according to the manufacturer's specifications, in most cases, synchronous machines will instantly trip at 47.5 Hz. Therefore, the frequency excursion process should not allow the frequency below that level to avoid the synchronous generators to trip, which might lead to possible blackouts. With the penetrations of renewable energy sources into the grid, the ROCOF becomes more sensitive and responsive to the disturbances. It is observed that the UFLS with conventional settings suitably works for distributed synchronous generators, but it fails to arrest frequency declination when the large-scale renewable energy sources are integrated into the grid. In Table 9, the comparison of conventional settings and proposed settings are summarized for different contingencies (44%, 20% and 8% of gen loss) based on the simulation results.

Table 9 Comparison between the proposed and conventional (Conv.) UFLS settings.

	Conv.	**Proposed**	**Conv.**	**Proposed**	**Conv.**	**Proposed**
Gen. loss (%)	44	44	20	20	8	8
Nadir Freq. (Hz)	46.91	47.88	48.48	48.56	49.51	49.51
Steady state Freq. (Hz)	49.43	49.5	50.42	49.52	4.51	49.51
Load shed (MW;MVAR)	166; 64.79	221; 86	166 ; 64.79	64; 27	None	None

From Table 9, it is observed that the conventional UFLS settings can easily arrest frequency declination without any renewable energy penetration. On the other hand, although the conventional UFLS settings successfully arrest frequency for 20% and 8% generation loss, they fail to arrest frequency for 44% generation loss even with 27% penetration of renewable energy. The nadir frequency falls below 47.5 Hz which may lead to a cascade tripping of remaining synchronous generators. This causes more imbalance between electricity generations and consumptions. The ROCOF becomes more severe in such condition which may lead to possible blackouts. However, the proposed load shedding scheme provides excellent outcomes for the given contingency conditions which allow the power system to survive from possible major blackouts. In fact, the proposed load shedding scheme is applicable to any contingency that makes the power system to be more robust to survive against any major blackouts. It is also worth mentioning that for middle contingencies the proposed load shedding scheme exerts less amount of load shedding than the conventional settings. But in case of higher contingencies (44% gen. loss), due to the steeper response of ROCOF, the proposed method executes more amount of load shedding though it is successful to restrict the frequency falling within 47.5Hz and thereby, avoiding blackouts.

To compare the performance of the proposed load shedding scheme this thesis includes another established method based on the mixed integer linear programming (MILP) [6]. Chapter 4 consists of the development of the MILP method to determine the load shedding scheme. For optimizing relay parameters, minimizing the amount of load shedding has been considered as an objective function. In [6] the performance of the MILP method was evaluated on a system with high strength but in this thesis, this method has been implemented on a comparatively low strength system. Finding deficiencies of this method on lower system inertia-based grid is one of the objectives of this thesis.

Chapter 4

4.1 Introduction

In this chapter, a mixed integer linear programming technique (MILP)[6] is implemented to set a under-frequency relay's parameter for avoiding blackouts in low-inertia based power grids (in this case on the test network). The performance of the MILP technique is tested for a network consisting of synchronous generators only [6]. But its performance was not tested in the presence of renewable energy sources in existing literatures. In this section, the performance of the MILP scheme is tested in the test network by performing three case studies (same as chapter 3 and 4).

4.2 Formulation of MILP to Extract Relay Parameters

4.2.1 Contingencies due to Generation losses

For a power system model containing ng generators, there may have $2^{ng} - 2$ contingencies (here 0% and 100% of generation losses are being ignored). In general, each generator can be addressed by the index i, a set of contingencies C_j can be considered where j denotes the contingency number, then the generation loss resulting from each contingency j is calculated by using the following equation:

$$\Delta g^j = \sum_{i \in C^j} g_i^0 \tag{4.1}$$

The equivalent system's inertia constant following j contingency is calculated as:

$$H^j = \sum_{i \notin C^j} H_i \tag{4.2}$$

where all values of H_i are expressed in $\frac{MJ}{MW}$. similarly, the equivalent governor droop value can be computed as:

$$\frac{1}{R^j} = \sum_{i \notin C^j} \frac{1}{R_i} \tag{4.3}$$

In this thesis, only three contingencies are considered ($J = 1, 2, 3$). Thus, the contingencies become:

$$C_1 = 44\ \%\ of\ gen\ loss,$$

$$C_2 = 20\%\ of\ gen\ loss\ and$$

$C_3 = 8\%\ of\ gen\ loss.$

4.2.2 Under-frequency/Time Limitations

As discussed above, for each generator there are specific frequency threshold limits and allowable time at these threshold limits. Though it varies from a manufacturer to

manufacturer, but according to IEEE guidelines for simulation the following settings are used (see Table 10).

Table 10 Typical generator off-nominal frequency/time limitations.

Under frequency limits(Hz)	Over frequency limits (Hz)	Maximum permissible time
50.5 – 49.5	50 – 50.5	N/A (continuous operation)
49.4-48.5	50.6-51.5	30 seconds – 3 minutes
48.4 -47.9	51.6 – 51.7	7.5 seconds
47.5 – 47.8		7.2 cycles
Less than 47.5	Greater than 61.7	Instantaneous trip

If for any ith generator the frequency falls below any of those threshold limits for equal or more than the defined time limits, then the generator will trip. Mathematically the logic can be written as:

If for any $l = 1, \dots, nl, f(t_0) = f_i^l \; and \; f(t) \leq f_i^l \; for \; t_0 \leq t \leq t_0 + \Delta t_i^l$ the trip generating unit i.

4.2.3 Models for Shedding Loads

Here the continuous load shedding model is assumed. Following the conventional load shedding scheme and PSS/E relay models, a three-stage load shedding is considered. In this case load shedding points, the amount of load shedding in each stage and the time limit before load shedding are to be decided with MILP program. Therefore, the decision variables {frequency shedding point (f_s) ,

time limit before load shedding (Δt_s),

amount of load shedding(Δd_s),

shedding stages, $s = 1,2,3$} are to be extracted from the MILP program.

4.2.4 Discrete Time-Frequency Response Model

From equation (1.9) it can be mentioned that each contingency must satisfy the following time-discretized frequency trajectory:

$$\Delta f_n^j = \Delta f_{n-1}^j + \Delta K_{n-1}^j \Delta t; \quad \forall j, n \tag{4.4}$$

where K_n^j is the frequency gradient which can be expressed by including the load shedding ($\Delta d_n = \sum_s u_{sn}^j \, \Delta d_s$), where u_{sn}^j is a binary variable which relates with the relay timer model and the relay operation logic are discussed in the next sub-section, and Δd_s is the amount of load shedding. Frequency gradient is calculated as:

$$K_n^j = \frac{f_0}{2H^j}\left(\Delta r_n^j - \Delta g^j + \sum_s u_{sn}^j \, \Delta d_s - D\Delta f_n^j\right); \forall j, n \tag{4.5}$$

While equation (1.11) takes the following form in discrete model

$$\Delta r_n^j = \Delta r_{n-1}^j + \frac{\Delta t}{T}\left(-\frac{\Delta f_n^j}{R^j} - \Delta r_{n-1}^j\right) \;\forall\, j, n \tag{4.6}$$

Note that equation (5.5) contains load shedding amount which is a product of binary variable and load shed Δd_s , which is not continuous in nature. For continuous load shedding model $\sum_s u_{sn}^j\, \Delta d_s$ can be replaced by another variable x_{sn}^j such that, it follows for all j, n:

$$0 \le x_{sn}^j \le u_{sn}^j \tag{4.7}$$

$$0 \le \Delta d_s - x_{sn}^j \le (1 - u_{sn}^j) \tag{4.8}$$

From the above equations, it is clear that when $u_{sn}^j = 1$ then $x_{sn}^j = \Delta d_s$, while when $u_{sn}^j = 0$ then $x_{sn}^j = 0$.

4.2.5 Relay Timer Model

Each frequency set point, f_s can be defined by putting a binary variable v_{sn}^j such that $v_{sn}^j = 0$ when frequency is above the frequency set point and $v_{sn}^j = 1$ for any frequency below the set point. Mathematically the linear inequality can be written as:

$$\frac{f_s - (f_0 + \Delta f_n^j)}{L} \le v_{sn}^j \le 1 + \frac{f_s - \left(f_0 + \Delta f_n^j\right)}{L};\; \forall\, s, j, n \tag{4.9}$$

where, L is a large number (e.g. 50). Total time below the set frequency limit can be estimated by the following linear equation:

$$\Delta t_{sn}^j = \Delta t_{s,n-1} + v_{sn}^j \Delta t;\; \forall\, s, j, n \tag{4.10}$$

4.2.6 Relay Operation Logic

As frequency trajectory cuts any set point for any defined time limit, relay must execute an amount of load shedding which will reduce the frequency decline. This condition can be implemented by putting another binary variable u_{sn}^j such that,

$$\frac{\Delta t_{sn}^j - \Delta t_s}{L} \le u_{sn}^j \le 1 + \frac{\Delta t_{sn}^j - \Delta t_s}{L};\; \forall\, s, j, n \tag{4.11}$$

Here $u_{sn}^j = 0$ when the time interval spent under the set point is below the set limit (Δt_s) and $u_{sn}^j = 1$ when time interval crosses or equal the time limit (Δt_s). L is a large positive number (e.g., 20). In case of conventional setting relay pick-up time is considered, about 0.2 sec. For simplicity in MILP relay pick-up time is considered $(\Delta t_s = 0.2 \text{ sec})$. So time limit before load shedding (Δt_s), is no longer a decision variable.

Any load which is shed during an under-frequency event cannot be restored again. This logic can be expressed by:

$$u_{sn}^{j} \geq u_{s,n-1}^{j};\ \forall\, s,j,n \tag{4.12}$$

In addition, to avoid different load shedding simultaneously, the following logic is used and given as:

$$\sum_{s} u_{sn}^{j} - \sum_{s} u_{s,n-1}^{j} \leq 1; \forall\, j,n \tag{4.13}$$

Finally, to consider load shedding priority, the following condition is enforced. Here, the higher the index s, the lower the priority of the corresponding load block.

$$u_{sn}^{j} \geq u_{s+1,n}^{j};\ \forall\, s,j,n \tag{4.14}$$

4.2.7 Stable Steady-State Frequency Condition

It is desired that at the end of frequency excursion process it should return to a safe limit (e.g., in this case, safe range is 49.5 Hz to 50.5 Hz). To limit the steady state frequency within that limit the following logic is made:

$$0.5 \leq \Delta f_{N}^{j} = \left(\frac{-\Delta g^{j} + \sum_{s} x_{sN}^{j}}{D + \frac{1}{R^{j}}} \right) \leq -0.5 \tag{4.15}$$

Here,

$N =$ The last time step in the simulation and

$x_{sN}^{j} =$ The total amount of load shed during trajectory j up to time N.

This condition also limits the possibility of the frequency overshoot at the end of the frequency excursion process.

4.2.8 Removing Oscillation in Steady-State Frequency Condition

At the end of the frequency recovery process, an oscillation is observed around the steady-state value. However, it can also be limited by the following linear inequality:

$$\varepsilon \geq \Delta f_{N}^{j} - \frac{1}{np} \sum_{np}^{N} \Delta f_{n}^{j} \geq -\varepsilon \tag{4.16}$$

where np is the last few steps (typically between 5 to 10 steps). The above equation deals with the average frequency deviations of the last 5- or 10-time steps.

4.2.9 Constraints for Load shedding Blocks

For continuous load shedding model, the following relation is considered:

$$\sum_{s} d_s \leq d \tag{4.17}$$

where d is the total system load demand, and d_s is the amount of each stage's load shedding.

4.2.10 Other Constraints of Frequency Set Point

As stated above, frequency set points are the decision variables for MILP, it should be put under certain boundaries. To do that the set points are bounded between the safest allowable lower limit of frequency (49.5 Hz) and the last threshold limit at which generators trip instantaneously (47.5 Hz). Mathematically the logic is:

$$\min\{f_l\} \leq f_s \leq f_{max} \tag{4.18}$$

Equal frequency set points can be avoided by the following condition:

$$f_s - f_{s+1} \geq \Delta f_{min} \tag{4.19}$$

The typical value of Δf_{min} is 0.2 Hz.

4.3 MILP Formulation

As stated above among three decision variables (frequency set points, relay pick up time, and the amount of load shedding in each stage), only relay pick up time is fixed (0.2 sec). Therefore, in this circumstance, there are two variables are left to decide. From the above section, it is seen that the UFLS problem consists of several variables (including binary) and complicated constraints. However, it can be solved using a commercial optimizer (GAMS), by setting an objective function as[6]:

$$obj = min\ \{\textstyle\sum_j (p^j \sum_s x_{s,N})\} \tag{4.20}$$

where p^j is the probability of occurring any contingencies, which can be estimated by employing a constant equal to 1 over the number of contingencies.

The objective function is minimized by using MIP solution in GAMS to extract relay parameters subject to the constraints from equations (4.1) to (4.19).

4.4 Simulation with MILP

Data from Table 3 have been used to determine the relay parameters by applying MILP program in GAMS (commercial optimizer software). It is assumed that all three contingencies discussed before (44% gen loss, 20% gen loss and 8% gen loss) have an equal probability of occurrence. The case study uses a governor time constant of 5 sec, while frequency set points are considered to be between 49.4 Hz to 47.9 Hz. A step size of 0.1 sec is used and as discussed earlier a time delay of 0.2 sec before load shedding is considered. Three load shedding stages with a steady state frequency deviation of

49.5 to 50.5 Hz are being considered. The solutions of minimum load shed are found in about 42 sec with a personal computer having the configuration of core i-7, 3.5 GHz processor.

Table 11 Relay Setting Parameters from MILP Formulations.

Frequency (Hz)	Load shed (in P.U)	Time Delay (Sec)
49.2	0.15	0.2
48.55	0.14	0.2
48.03	0.07	0.2

After putting this setting, the case studies described in Section 4 are checked again to see the performance of this scheme.

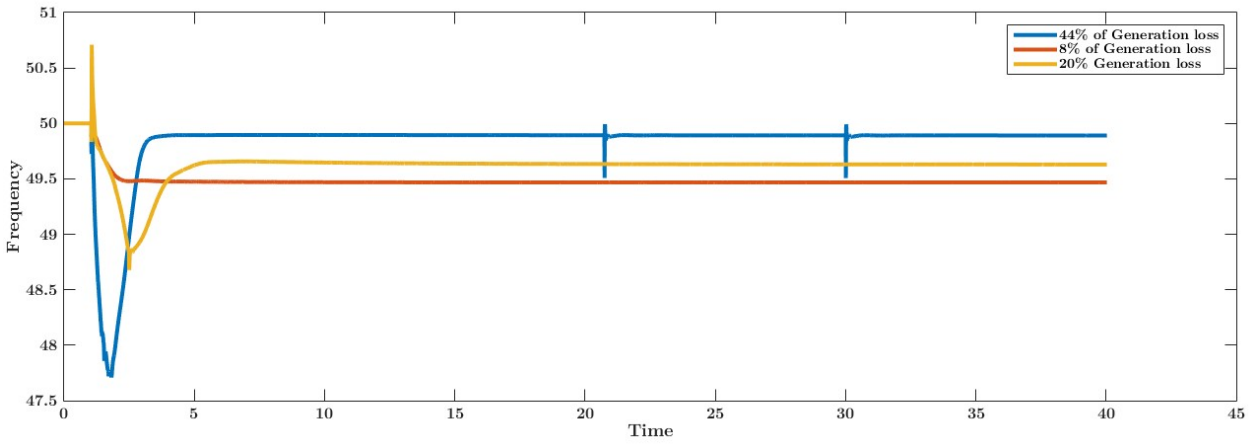

Figure 24 Frequency responses following different contingencies with MILP settings.

The above figure shows that under-frequency relay complies with all the criteria's of under-frequency load shedding (described in (5.1.1) to (5.1.10)) in all three contingencies. It is noted that, so far it is being considered that loads are static i.e. we have used an average load of those feeders. But with time and seasons, these loads vary. Any predefined off-line UFLS settings rely on average load estimation. But there is a possibility of occurring frequency undershoot at a certain moment when the feeder loads are less than the average loads, resulting insufficient load shedding. Any predefined setting in feeder Therefore, any off-line UFLS settings (including conventional and MILP) has a major drawback regarding the variation of loads.

Chapter 5

5.1 Results and Discussion

From the discussion of Chapter 5 and Chapter 3, it is clear that all the calculations for relay parameter's setting are based on a percentage of generation losses, machines data etc. But the execution of that settings relies on the connected loads which may vary with time. For this reason, insufficient load shedding may occur with the off-line methods ofan UFLS scheme. Whereas, in the on-line method of an UFLS scheme load shedding amount and feeder to be shed are decided by the instant power deflection which will try to avoid excess or less load shedding and successfully bring back the frequency within the desired state.

5.2 Comparisons of Different UFLS Schemes

For comparison and analysis of the performance of two off-line (conventional and MILP) and one online (Proposed load shedding scheme), only one contingency which is 44% generation loss (as in the conventional scheme maximum protection scheme is considered for 50% of generation loss) is observed.

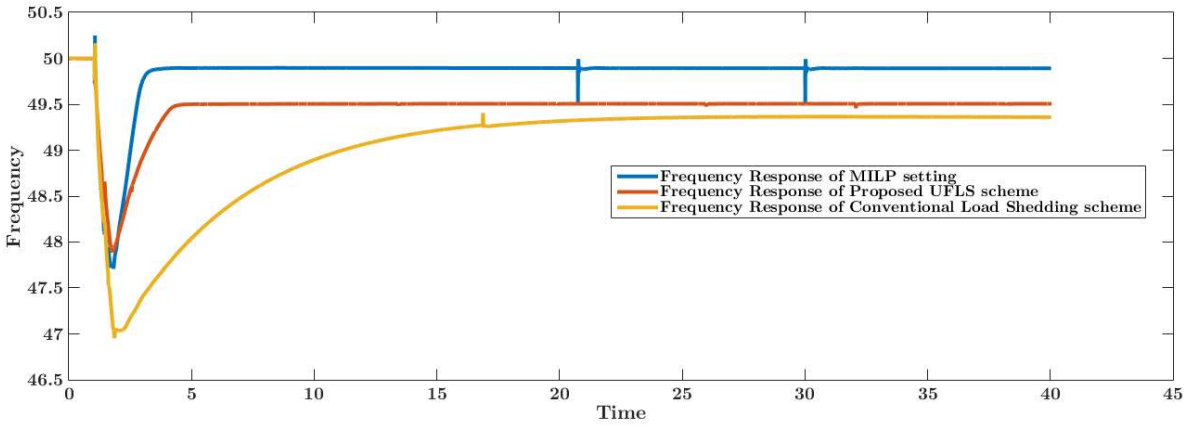

Figure 25 Frequency responses following 44% of generation loss.

Figure 22 depicts that both the proposed and MILP UFLS scheme successfully restrict frequency excursion above the threshold limits (47.5 Hz). But conventional load shedding scheme fails to do so. In this case or worse conditions conventional load shedding scheme can cause cascade tripping of the remaining synchronous generators which will increase more frequency decline leading to system blackouts. In addition to that, the conventional scheme fails to bring frequency back to stable steady-state conditions, which is in between 49.5 to 50.5 Hz. Below 49.5 Hz, a synchronous

generator can sustain until 30 sec to 3 minutes (see Table 2). After that, the generator protection system will disconnect the generator from the grid and causes more generation losses. Furthermore, a conventional UFLS scheme takes more than 20 seconds to achieve the steady state condition while both the proposed and MILP UFLS scheme require less than 5 seconds to achieve the steady state condition. Moreover, for the worst contingency (i.e. 44% of gen loss) conventional scheme costs 166 MW load shed and the MILP and proposed UFLS scheme cost 215 MW and 221 MW load shedding in the process of frequency excursion process. In this sense, MILP shows better performance than the conventional and proposed UFLS scheme. So far loads are considered static but in reality, they change with time. Due to the uncertainty of loads, a predefined load shed amount may fail to protect the frequency excursion process. On the other hand, online-based proposed load shedding scheme assesses the load shedding amount on basis of instant power deficits and execute load shedding accordingly. Therefore, with the proper distribution of loads to be shed, insufficient load shedding can be avoided. For the distribution load shedding, feeders can be selected by a PSO based optimization. An optimized load shedding will make the performance of the proposed scheme better. With the proposed UFLS scheme, the risk of blackouts due to insufficient load shedding can be minimized.

Again, in the case of 20% generation loss, conventional scheme proves to be costlier than the MILP and proposed load shedding scheme. For this reason, traditional scheme exhibits a steady state frequency which is more than 50 Hz (50.42 Hz exactly). In another word, it can be mentioned that a small overshoot has been noticed at the end of an UFLS event which can be avoided by using any one of the two schemes. It is noteworthy that, the proposed scheme is designed to get a steady state frequency of 49.5 Hz, and MILP setting achieves the steady state frequency at 49.63 Hz. Moreover, the proposed scheme costs less load shedding than the traditional and MILP scheme on such a medium contingency.

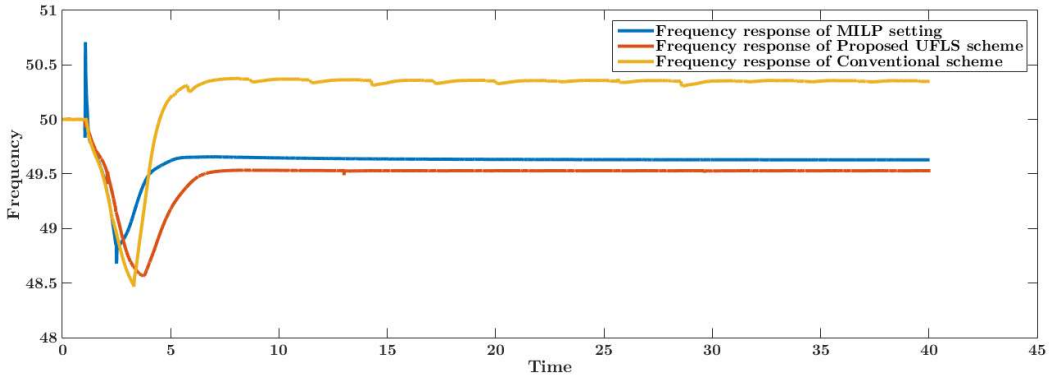

Figure 26 Frequency responses following 20% of generation loss.

For the lowest contingency (8% of generation loss), no load shedding is needed for any of these described load shedding strategies (see Figure 24). So, it can be concluded that lowest contingency has less concern than the medium and worst contingency.

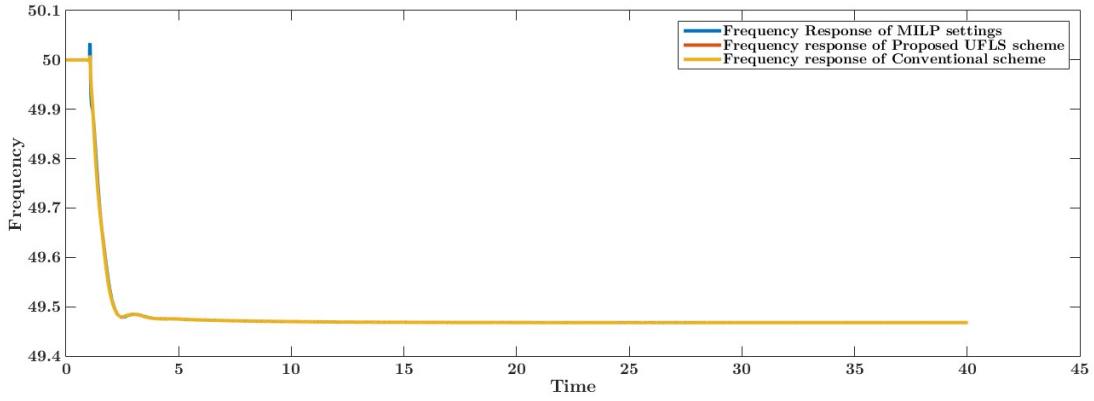

Figure 27 Frequency responses following 20% of generation loss.

A comparison table has been shown to show the differences in the three load shedding strategies (traditional, MILP and the proposed UFLS scheme) in terms of nadir, steady-state frequency, and load shedding amounts

Table 12 Comparison chart of Conventional, Proposed and MILP UFLS scheme.

	Conv.	**Proposed**	**MILP**	**Conv.**	**Proposed**	**MILP**	**Conv.**	**Proposed**	**MILP**
Gen. loss (%)	44	44	44	20	20		8	8	
Nadir Freq. (Hz)	46.91	47.88	47.72	48.48	48.56	48.70	49.51	49.51	49.51
Steady state Freq. (Hz)	49.43	49.5	49.89	50.42	49.52	49.63	4.51	49.51	49.51
Load shed (MW;MVAR)	166; 64.79	221; 86	215.03; 76.03	166 ; 64.79	64; 27	77; 29.79	None	None	None

Chapter 6

6.1 Conclusion

The proposed UFLS scheme is based on the detection of the power deficit from the ROCOF. In order to minimize the amount of load shedding and keep the steady state frequency within the acceptable limits, the total system's damping factor is considered to calculate the amount of load shedding. Using the ROCOF to determine the load-shedding amount is one of the methods of calculating the amount of actual power imbalance. The conventional UFLS scheme and the proposed UFLS scheme are applied to a test network. The simulations are carried out by using Python-based PSS/E simulator. The deficiencies of the conventional UFLS scheme are analyzed and a modified UFLS scheme is proposed to overcome the shortcomings of the problems related to the conventional scheme. Then, the mixed integer linear program (MILP) is used to extract relay parameters. The performances of MILP are tested to compare with the proposed UFLS model and the traditional ones. Moreover, the frequency response and amount of load shedding are compared with the MILP and the proposed UFLS scheme to evaluate the performance. In this thesis, load shedding is carried out randomly, however, a priority based optimized load-shedding scheme may provide better performance.

6.2 Achievements

One of the major reasons for the blackouts is insufficient load shedding, where relays are predefined with a fixed amount of load to be shed at certain frequency levels. Moreover, the replacements of synchronous generators by the renewable energy sources. System frequency gets more responsive following any contingency due to a low system's inertia. ROCOF is getting more severe and the risk of more generation losses becomes higher with the penetrations of renewable energy sources. The proposed load shedding scheme is an online based scheme which decides the load curtail amounts on the basis of instant power deficits. The conventional or MILP scheme[6] has predefined settings for load shedding in which the risk of insufficient load shedding during the frequency excursion process remains the same. In addition, the conventional scheme fails to protect frequency decline below the threshold limits causing a further trip of remaining generators. Online based proposed UFLS scheme considers those facts and prove to be more effective to minimize the risks of possible blackouts. Moreover, by considering the total system's damping factor, the load shedding method is slightly modified from the one given in [48]. This improved method results less load shedding compare to the method described in [48]. Steady-state frequency can be controlled with the proposed scheme so an undesirable overshoot at the end of UFLS process can be eliminated.

6.3 Future Works

The risks of blackouts increase with the decrease of a grid's inertia. The online based UFLS schemes are proven to be effective so far for the low inertia-based system grid. Determining the amount of load to be shed utilizing real-time information can be one of the best ways to bring back frequency into safe limits. But load curtailment is not the best solution for a system in terms of reliability. It affects the system's SAIDI and SAIFI and degrades the quality of electricity supply. The importance of using renewable energy sources is undeniable due to their inexhaustability and non polluting nature. But at the same time efficient measures should be taken so that this doesn't affect overall system stability. This thesis represents a probable solution to maintain system stability of a low strength grid using the concept of on-line based under frequency load shedding technique. Yet, like all other methods, the proposed method also has some areas which demand further improvements. Since the proposed UFLS scheme is based on on-line based measurement and communication system, any error due to communcation system may affect the process of determining the amount of load shedding. Furthermore, in this paper, load shedding is carried out randomly, however, a priority based optimized load-shedding scheme may provide better performance. Besides, the following works on low inertia based power grid can be some other promising solutions.

a. Modeling of low inertia based power grid by using the battery as external energy sources to support the power shortage such that, ROCOF remain acceptable limit.
b. The synthetic inertia of the wind turbine can be a good solution for frequency stability again it needs to satisfy all type of contingencies in a low inertia based system grid.
c. Contributions on system strength by using modularity of grid-connected converter.
d. Improving system strength by virtual synchronous generator by using supplementary controller specifically derivative & propotional controller.

Reference

[1] "Wikipedia." [Online]. Available: https://en.wikipedia.org/wiki/List _of_major_power_outage.

[2] T. Güler and G. Gross, "The economic evaluation of system security criterion selection in the market environment," in *IEEE PES General Meeting*, 2010, pp. 1–8.

[3] M. Ghaderi Darebaghi and T. Amraee, "Dynamic multi-stage under frequency load shedding considering uncertainty of generation loss," *IET Gener. Transm. Distrib.*,

vol. 11, no. 13, pp. 3202–3209, Sep. 2017.

[4] D. Yang, S. Liu, and G. Cai, "Optimal System Frequency Response Model and UFLS Schemes for a Small Receiving-End Power System after Islanding," pp. 8–13, 2017.

[5] "Today in SA: blackout cost $367m but could have been worse." [Online]. Available: https://www.theaustralian.com.au/national-affairs/state-politics/today-in-sa-blackout-cost-367m-but-could-have-been-worse/news-story/f9250bc56e0423b582ca9bd9f1c92e6e. [Accessed: 02-Aug-2018].

[6] F. Ceja-Gomez, S. S. Qadri, and F. D. Galiana, "Under-Frequency Load Shedding Via Integer Programming," *IEEE Trans. Power Syst.*, vol. 27, no. 3, pp. 1387–1394, Aug. 2012.

[7] Y. G. Rebours, D. S. Kirschen, M. Trotignon, and S. Rossignol, "A survey of frequency and voltage control ancillary services - Part I: Technical features," *IEEE Trans. Power Syst.*, vol. 22, no. 1, pp. 350–357, Feb. 2007.

[8] IEEE Power Engineering Society. Power Systems Relaying Committee., Institute of Electrical and Electronics Engineers., and IEEE-SA Standards Board., *IEEE guide for the application of protective relays used for abnormal frequency load shedding and restoration*. Institute of Electrical and Electronics Engineers, 2007.

[9] V. V. Terzija and H.-J. Koglin, "Adaptive underfrequency load shedding integrated with a frequency estimation numerical algorithm," *IEE Proc. - Gener. Transm. Distrib.*, vol. 149, no. 6, p. 713, 2002.

[10] P. M. Anderson and M. Mirheydar, "An adaptive method for setting underfrequency load shedding relays," *IEEE Trans. Power Syst.*, vol. 7, no. 2, pp. 647–655, May 1992.

[11] J. Duncan Glover, *Power system analysis and design J. Duncan Glover, Mulukutia S. Sarma, Thomas J. Overbye [electronic resource] - Version details - Trove*, 5th ed. Stamford, CT Cengage Learning 2012, 2012.

[12] A. Gjukaj, G. Kabashi, G. Pula, N. Avdiu, and B. Prebreza, "Re-Design of Load Shedding Schemes of the Kosovo Power System," vol. 5, no. 2, pp. 156–160, 2011.

[13] J. Restrepo and F. Galiana, "Unit commitment with primary frequency regulation constraints," in *2006 IEEE Power Engineering Society General Meeting*, 2006, p. 1 pp.

[14] "The Australian." [Online]. Available: https://www.theaustralian.com.au/national-affairs/state-politics/today-in-sa-blackout-cost-367m-but-could-have-been-worse/news story. [Accessed: 09-Aug-2018].

[15] S. Nourollah, A. Pirayesh, and F. Aminifar, "Combinational scheme for voltage and frequency recovery in an islanded distribution system," *IET Gener. Transm. Distrib.*, vol. 10, no. 12, pp. 2899–2906, Sep. 2016.

[16] F. Sayed, S. Kamel, and O. Abdel-Rahim, "Load shedding solution using multi-objective teaching-learning-based optimization," in *2018 International Conference on*

Innovative Trends in Computer Engineering (ITCE), 2018, pp. 447–452.

[17] M. Karimi, R. Azizipanah-Abarghooee, H. Uppal, Q. Hong, C. Booth, and V. Terzija, "Smart integrated adaptive centralized controller for islanded microgrids under minimized load shedding," in *2017 5th International Istanbul Smart Grid and Cities Congress and Fair (ICSG)*, 2017, pp. 41–45.

[18] M. Ghaderi Darebaghi and T. Amraee, "Dynamic multi-stage under frequency load shedding considering uncertainty of generation loss," *IET Gener. Transm. Distrib.*, vol. 11, no. 13, pp. 3202–3209, Sep. 2017.

[19] U. Rudez and R. Mihalic, "WAMS-Based Underfrequency Load Shedding With Short-Term Frequency Prediction," *IEEE Trans. Power Deliv.*, vol. 31, no. 4, pp. 1912–1920, Aug. 2016.

[20] A. Ketabi and M. H. Fini, "An Underfrequency Load Shedding Scheme for Hybrid and Multiarea Power Systems," *IEEE Trans. Smart Grid*, vol. 6, no. 1, pp. 82–91, Jan. 2015.

[21] D. Cai, H. Ju, H. Ma, and L. Ding, "Smart frequency control schemes in distribution network with renewable resources," in *2014 IEEE PES Asia-Pacific Power and Energy Engineering Conference (APPEEC)*, 2014, pp. 1–5.

[22] E. Gholipour, G. Isazadeh, and A. Khodabakhshian, "New intelligent controlled islanding scheme in large interconnected power systems," *IET Gener. Transm. Distrib.*, vol. 9, no. 16, pp. 2686–2696, Dec. 2015.

[23] Qian Liu, L. Ding, Yichen Guo, Zhenbin Ma, and Daonong Zhang, "A controlled islanding scheme considering stability margin of sub-systems after splitting," in *2016 IEEE PES Asia-Pacific Power and Energy Engineering Conference (APPEEC)*, 2016, pp. 531–535.

[24] S. Soman, P. Thomas, J. George, and Ganesh M., "Prevention of blackout by an effective forced islanding and restoration scheme," in *2015 International Conference on Emerging Research in Electronics, Computer Science and Technology (ICERECT)*, 2015, pp. 298–303.

[25] V. Muzik and V. Vajnar, "Frequency and voltage stability assessment of a power system during emergency service states," in *2018 IEEE Conference of Russian Young Researchers in Electrical and Electronic Engineering (EIConRus)*, 2018, pp. 708–711.

[26] U. Datta, A. Kalam, and J. Shi, "Battery energy storage system for transient frequency stability enhancement of a large-scale power system," in *2017 Australasian Universities Power Engineering Conference (AUPEC)*, 2017, pp. 1–5.

[27] H. T. Nguyen, G. Yang, A. H. Nielsen, and P. H. Jensen, "Frequency stability enhancement for low inertia systems using synthetic inertia of wind power," in *2017 IEEE Power & Energy Society General Meeting*, 2017, pp. 1–5.

[28] J. Wang, H. Zhang, and Y. Zhou, "Intelligent Under Frequency and Under Voltage

Load Shedding Method Based on the Active Participation of Smart Appliances," *IEEE Trans. Smart Grid*, vol. 8, no. 1, pp. 353–361, Jan. 2017.

[29] K. U. Z. Mollah and N.-K. C. Nair, "Adaptive market based load shedding scheme," in *2015 IEEE Power & Energy Society General Meeting*, 2015, pp. 1–5.

[30] W. Gu *et al.*, "Adaptive Decentralized Under-Frequency Load Shedding for Islanded Smart Distribution Networks," *IEEE Trans. Sustain. Energy*, vol. 5, no. 3, pp. 886–895, Jul. 2014.

[31] E. J. Thalassinakis, E. N. Dialynas, and D. Agoris, "Method Combining ANNs and Monte Carlo Simulation for the Selection of the Load Shedding Protection Strategies in Autonomous Power Systems," *IEEE Trans. Power Syst.*, vol. 21, no. 4, pp. 1574–1582, Nov. 2006.

[32] Y. Lu, W.-S. Kao, and Y.-T. Chen, "Study of Applying Load Shedding Scheme With Dynamic<tex>$rm D$</tex>-Factor Values of Various Dynamic Load Models to Taiwan Power System," *IEEE Trans. Power Syst.*, vol. 20, no. 4, pp. 1976–1984, Nov. 2005.

[33] *Power system stability and control / P. Kundur ; edited by Neal J. Balu, Mark G. Lauby. - Version details - Trove.* .

[34] F. Shokooh *et al.*, "An intelligent load shedding (ILS) system application in a large industrial facility," in *Fourtieth IAS Annual Meeting. Conference Record of the 2005 Industry Applications Conference, 2005.*, vol. 1, pp. 417–425.

[35] S. Industry, S. Power, and T. International, "Pss ® e 33.4 m," 2013.

[36] L. Yao, W.-C. Chang, and R.-L. Yen, "An Iterative Deepening Genetic Algorithm for Scheduling of Direct Load Control," *IEEE Trans. Power Syst.*, vol. 20, no. 3, pp. 1414–1421, Aug. 2005.

[37] "Weblet Importer." [Online]. Available: https://pgcb.org.bd/PGCB/user/grid-network.php. [Accessed: 13-Aug-2018].

[38] M. J. Hossain, H. R. Pota, M. A. Mahmud, and R. A. Ramos, "Investigation of the Impacts of Large-Scale Wind Power Penetration on the Angle and Voltage Stability of Power Systems," *IEEE Syst. J.*, vol. 6, no. 1, pp. 76–84, Mar. 2012.

[39] B. Pal and B. Chaudhuri, *Robust control in power systems*. Springer, 2005.

[40] "Load representation for dynamic performance analysis (of power systems)," *IEEE Trans. Power Syst.*, vol. 8, no. 2, pp. 472–482, May 1993.

[41] X. Wang and M. Yue, "Design of Energy Storage System to Improve Inertial Response for Large Scale PV Generation," 2016.

[42] *POM_PSSE33.pdf.* .

[43] "Dynamic Modelling of a Solar PV Plant on PSSE | Write-Ups of Supun De Silva." [Online]. Available: https://supundesilva.blogspot.com/2014/08/dynamic-modelling-

solar-pv-plant-on-psse.html. [Accessed: 13-Aug-2018].

[44] J. Jallad, S. Mekhilef, H. Mokhlis, and J. A. Laghari, "Improved UFLS with consideration of power deficit during shedding process and flexible load selection," *IET Renew. Power Gener.*, vol. 12, no. 5, pp. 565–575, Apr. 2018.

[45] H. Mohamad, S. Sahdan, N. N. Y. Dahlan, and N. M. Sapari, "Under-frequency load shedding technique considering response based for islanding distribution network connected with mini hydro," in *2014 IEEE 8th International Power Engineering and Optimization Conference (PEOCO2014)*, 2014, pp. 488–493.

[46] A. Ketabi and M. Hajiakbari Fini, "An underfrequency load shedding scheme for islanded microgrids," *Int. J. Electr. Power Energy Syst.*, vol. 62, pp. 599–607, Nov. 2014.

[47] IEEE-SA Standards Board., IEEE Power Engineering Society. Power Systems Relaying Committee., and Institute of Electrical and Electronics Engineers., *IEEE guide for abnormal frequency protection for power generating plants*. Institute of Electrical and Electronics Engineers, 2004.

[48] J. Jallad, S. Mekhilef, H. Mokhlis, and J. A. Laghari, "Improved UFLS with consideration of power deficit during shedding process and flexible load selection," *IET Renew. Power Gener.*, vol. 12, no. 5, pp. 565–575, Apr. 2018.

Appendix-A

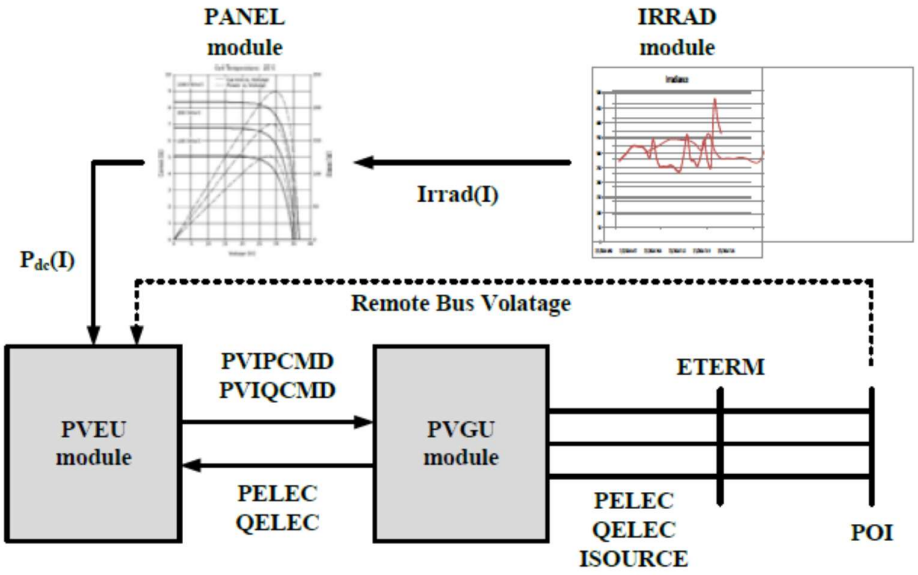

Figure 28 Interaction diagram of PV module with grid[41]

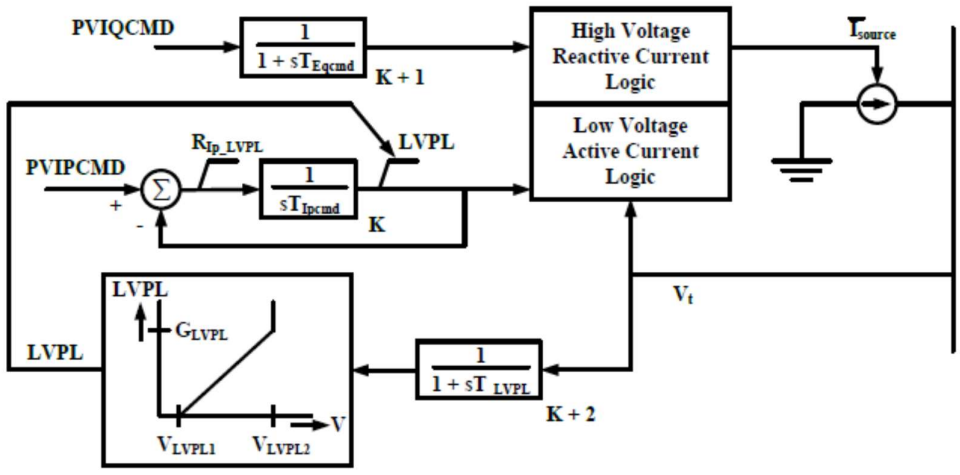

Figure 29 PVGU model in PSS/E[41]

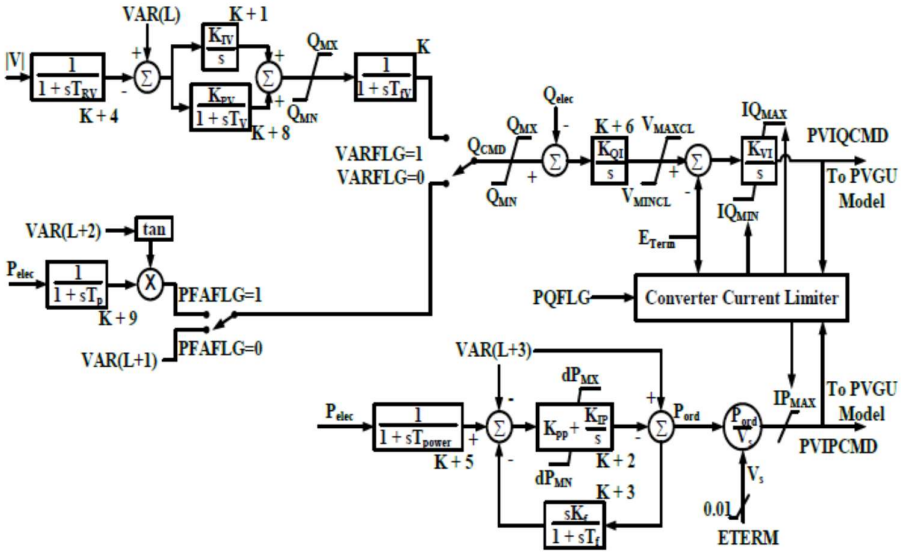

Figure 30 PVEU module in PSS/E[41]

PVGU1

TIQCmd, Converter time constant for IQcmd, second	0.02
TIpCmd, Converter time constant for IPcmd, second	0.02
VLVPL1 - Low Voltage power Logic (LVPL), voltage 1 (pu)	0.4
VLVPL2 - LVPL voltage 2 (pu)	0.9
GLVPL - LVPL gain	1.11
High Voltage reactive Current (HVRC) logic,voltage (pu)	1.2
CURHVRCR - HVRC logic, current (pu)	2
RIp_LVPL, Rate of active current change	2
T_LVPL, Voltage sensor for LVPL, second	0.02

PVEU1

Tfv - V-regulator filter	0.15
Kpv - V-regulator proportional gain	18
Kiv - V-regulator integrator gain	5
Kpp - T-regulator proportional gain	0.05
Kip - T-regulator integrator gain	0.1
Kf - Rate feedback gain	0
Tf - Rate feedback time constant	0.08
QMX - V-regulator max limit	0.47
QMN - V-regulator min limit	-0.47
IPMAX - Max active current limit	1.1
TRV - V-sensor	0
dPMX - Max limit in power PI controller (pu)	0.5
dPMN - Min limit in power PI controller (pu)	-0.5
T_POWER - Power filter time constant	0.05
KQi - MVAR/Volt gain	0.1
VMINCL	0.9

VMAXCL	1.1
KVi - Volt/MVAR gain	120
Tv - Lag time constant in WindVar controller	0.05
Tp - Pelec filter in fast PF controller	0.05
ImaxTD - Converter current limit	1.7
Iphl - Hard active current limit	1.11
Iqhl - Hard reactive current limit	1.11
PMAX of PV plant	64

PANELU1

P200, PDCmax at 200 W/m2, pu	0.16
P400, PDCmax at 400 W/m2, pu	0.38
P600, PDCmax at 600 W/m2, pu	0.59
P800, PDCmax at 800 W/m2, pu	0.85
P1000, PDCmax at 1000 W/m2, pu	1

IRRADU1

T1, Time of the first data point, second	5
I1, Irradiance at first data point, W/m2	1000
T2, Time of the second data point, second	10
I2, Irradiance at second data point, W/m2	900
T3, Time of the third data point, second	15
I3, Irradiance at third data point, W/m2	850
T4, Time of the fourth data point, second	20
I4, Irradiance at fourth data point, W/m2	800
T5, Time of the fifth data point, second	25
I5, Irradiance at fifth data point, W/m2	700
T6, Time of the sixth data point, second	30
I6, Irradiance at sixth data point, W/m2	600
T7, Time of the seventh data point, second	35
I7, Irradiance at seventh data point, W/m2	700
T8, Time of the eigth data point, second	0
I8, Irradiance at eigth data point, W/m2	0
T9, Time of the ninth data point, second	0
I9, Irradiance at ninth data point, W/m2	0
T10, Time of the tenth data point, second	0
I10, Irradiance at tenth data point, W/m2	0